



**HAL**  
open science

# Inorganic and organic carbon and nitrogen uptake strategies of picoplankton groups in the northwestern Atlantic Ocean

Hugo Berthelot, Solange Duhamel, Stéphane L'Helguen, Jean-françois Maguer, Nicolas Cassar

► **To cite this version:**

Hugo Berthelot, Solange Duhamel, Stéphane L'Helguen, Jean-françois Maguer, Nicolas Cassar. Inorganic and organic carbon and nitrogen uptake strategies of picoplankton groups in the northwestern Atlantic Ocean. *Limnology and Oceanography*, 2021, 66 (10), pp.3682-3696. 10.1002/lno.11909 . hal-03827246

**HAL Id: hal-03827246**

**<https://hal.science/hal-03827246v1>**

Submitted on 24 Oct 2022

**HAL** is a multi-disciplinary open access archive for the deposit and dissemination of scientific research documents, whether they are published or not. The documents may come from teaching and research institutions in France or abroad, or from public or private research centers.

L'archive ouverte pluridisciplinaire **HAL**, est destinée au dépôt et à la diffusion de documents scientifiques de niveau recherche, publiés ou non, émanant des établissements d'enseignement et de recherche français ou étrangers, des laboratoires publics ou privés.

1 Inorganic and organic carbon and nitrogen uptake strategies of  
2 picoplankton groups in the northwestern Atlantic Ocean

3 Hugo Berthelot<sup>1,4</sup>, Solange Duhamel<sup>2,5</sup>, Stéphane L'Helguen<sup>1</sup>, Jean-François Maguer<sup>1</sup>, Nicolas  
4 Cassar<sup>1,3</sup>

5 <sup>1</sup>Laboratoire des Sciences de l'Environnement Marin (LEMAR), UMR 6539  
6 UBO/CNRS/IRD/IFREMER, Institut Universitaire Européen de la Mer (IUEM), Brest, France.

7 <sup>2</sup>Lamont-Doherty Earth Observatory, Division of Biology and Paleo Environment, PO Box 1000, 61  
8 Route 9W, Palisades, NY 10964, USA.

9 <sup>3</sup>Division of Earth and Ocean Sciences, Nicholas School of the Environment, Duke University, Durham,  
10 NC 27708, USA.

11 <sup>4</sup>Now at: Sorbonne Université, CNRS, Station Biologique de Roscoff, AD2M, UMR 7144, Roscoff,  
12 France.

13 <sup>5</sup>Now at: Department of Molecular and Cellular Biology, The University of Arizona, Tucson, AZ 85721,  
14 USA.

15 Email addresses: H.B.: [hugo.berthelot@univ-brest.fr](mailto:hugo.berthelot@univ-brest.fr). S.D.: [duhamel@arizona.edu](mailto:duhamel@arizona.edu).

16 S.L.: [stephane.lhelguen@univ-brest.fr](mailto:stephane.lhelguen@univ-brest.fr). J.-F.M.: [jean-francois.maguer@univ-brest.fr](mailto:jean-francois.maguer@univ-brest.fr).

17 N.C.: [nicolas.cassar@duke.edu](mailto:nicolas.cassar@duke.edu)

18 Corresponding authors: Hugo Berthelot & Nicolas Cassar

19 Key words: Picoplankton, Nitrogen, Carbon, Leucine, Nitrate, Ammonium, Urea, *Prochlorococcus*,  
20 *Synechococcus*, nanoSIMS.

21 Running title: C and N uptake in picoplankton groups

22 Author contributions: H.B. and S. L. designed the experiment, H.B. carried the experiment. H.B., S.D.,  
23 S.L. and J.-F.M. participated in the analyses. N.C. supervised the project. All authors contributed to  
24 the interpretation of the results. H.B. wrote the manuscript with inputs from all the coauthors.

## 25 **Abstract**

26 Picoplankton populations dominate the planktonic community in the surface oligotrophic ocean. Yet,  
27 their strategies in the acquisition and the partitioning of organic and inorganic sources of nitrogen (N)  
28 and carbon (C) are poorly described. Here, we measured at the single-cell level the uptake of dissolved  
29 inorganic C (C-fixation), C-leucine, N-leucine, nitrate ( $\text{NO}_3^-$ ), ammonium ( $\text{NH}_4^+$ ) and N-urea in  
30 pigmented and non-pigmented picoplankton groups at six low-N stations in the northwestern Atlantic  
31 Ocean. Our study highlights important differences in trophic strategies between *Prochlorococcus*,  
32 *Synechococcus*, photosynthetic pico-eukaryotes and non-pigmented prokaryotes. Non-pigmented  
33 prokaryotes were characterized by high leucine uptake rates, non-significant C-fixation and relatively  
34 low  $\text{NH}_4^+$ , N-urea and  $\text{NO}_3^-$  uptake rates. Non-pigmented prokaryotes contributed to  $7\pm 3\%$ ,  $2\pm 2\%$  and  
35  $9\pm 5\%$  of the  $\text{NH}_4^+$ ,  $\text{NO}_3^-$  and N-urea community uptake, respectively. In contrast, pigmented groups  
36 displayed relatively high C-fixation rates,  $\text{NH}_4^+$  and N-urea uptake rates, but lower leucine uptake rates  
37 than non-pigmented prokaryotes. *Synechococcus* and photosynthetic pico-eukaryotes  $\text{NO}_3^-$  uptake rates  
38 were higher than *Prochlorococcus* ones. Pico-sized pigmented groups accounted for a significant  
39 fraction of the community C-fixation ( $63\pm 27\%$ ),  $\text{NH}_4^+$  uptake ( $47\pm 27\%$ ),  $\text{NO}_3^-$  uptake ( $62\pm 49\%$ ) and N-  
40 urea uptake ( $81\pm 35\%$ ). Interestingly, *Prochlorococcus* and photosynthetic pico-eukaryotes showed a  
41 greater reliance on C- and N- leucine than *Synechococcus* on average, suggesting a greater reliance on  
42 organic C and N sources. Taken together, our single-cell results decipher the wide diversity of C and N  
43 trophic strategies between and within marine picoplankton groups, but a clear partitioning between  
44 pigmented and non-pigmented groups still remains.

## 45 **Introduction**

46 Primary production is limited by nitrogen (N) availability in large portions of the world ocean (Moore  
47 et al. 2013). The scarcity of N resources selects for smaller phytoplankton with larger surface-area-to-

48 volume ratio. This strategy is believed to explain the biomass dominance of picoplankton ( $< 3 \mu\text{m}$ ) in  
49 oligotrophic regions (Marañón 2015). Picoplankton encompass a great diversity of populations and  
50 ecological functions (Massana 2011) but when analyzed using flow cytometry the populations generally  
51 cluster in well-defined groups including the pigmented photosynthetic groups of prokaryotes  
52 *Prochlorococcus* and *Synechococcus* and pico-eukaryotes, as well as the non-pigmented prokaryotes.  
53 These groups are present in the surface ocean in variable abundances and proportions depending on  
54 environmental factors such as temperature, light and nutrient supply (Otero-Ferrer et al. 2018).  
55 *Prochlorococcus* is present at latitudes lower than  $45^\circ\text{N/S}$  and numerically dominates the phytoplankton  
56 communities in oligotrophic and warm waters such as the subtropical gyres. *Synechococcus* is more  
57 widespread and is observed in nearly all the surface waters of the world ocean with the exception of the  
58 Arctic and Southern Oceans. As opposed to *Prochlorococcus*, *Synechococcus* is most abundant in  
59 temperate and relatively mesotrophic waters (Flombaum et al. 2020). Photosynthetic pico-eukaryotes  
60 are ubiquitous in the oceans and their biomass generally dominate over *Prochlorococcus* and  
61 *Synechococcus* in nutrient rich water and at high latitudes (Flombaum et al. 2020). They harbor a great  
62 diversity of organisms (including Prasinophyceae, Mamiellophyceae, Haptophyceae, Chrysophyceae,  
63 Pelagophyceae) making this group heterogeneous (Hernández-Ruiz et al. 2018; Mucko et al. 2018).  
64 Non-pigmented prokaryotes in surface layers of the oceans are also diverse, mostly composed of bacteria  
65 ( $>90\%$ ) (Ibarbalz et al. 2019), which are ubiquitous in the ocean at relatively high abundances ( $10^5$ - $10^6$   
66 cells  $\text{ml}^{-1}$ ) (Du et al. 2006).

67 Pigmented groups have traditionally been hypothesized to exclusively use dissolved inorganic carbon  
68 (C) as their source of C, and sunlight as a source of energy to fix C via photosynthesis (photoautotrophy).  
69 Conversely, non-pigmented prokaryotes are conventionally described as pure heterotrophs, i.e. relying  
70 on organic C for their growth, playing a key role in the remineralization of organic matter (Azam 1998).  
71 However, this idealized conceptual model is questioned by a growing body of evidence showing that  
72 mixed trophic regimes are a common feature in the ocean. Some pigmented organisms use organic C as  
73 sources of C and energy in addition to dissolved inorganic C, a trophic strategy called mixotrophy. The  
74 organic C acquisition can be mediated by a direct uptake of dissolved compounds (osmo-mixotrophy)

75 or by predation on prey (phago-mixotrophy) (Sanders and Gast 2012; Hartmann et al. 2012; Muñoz-  
76 Marín et al. 2020). Recent studies have demonstrated the high affinities of several pigmented species  
77 for dissolved organic substances, leading to a potential for resource competition with pure heterotrophs  
78 (Kamjunke et al. 2008). As an example, the complete gene pathways for glucose acquisition, and small  
79 but significant uptake rates have recently been found in *Prochlorococcus* and *Synechococcus* (Muñoz-  
80 Marín et al. 2020). Similarly, the use of dissolved inorganic C by non-pigmented organisms through  
81 chemoautotrophic processes has been reported in communities present in oceanic surface waters  
82 (Middelburg 2011).

83 This partitioning between organic and inorganic resources is also relevant to N acquisition. While the  
84 former traditional view is that pigmented organisms mostly rely on inorganic N, mainly ammonium  
85 ( $\text{NH}_4^+$ ) and nitrate ( $\text{NO}_3^-$ ), and non-pigmented prokaryotes on organic N substrates, including amino-  
86 acids, a number of studies have shown that the N strategies between the two trophic regimes are not  
87 completely distinct. In the N-rich sub-Arctic Pacific, non-pigmented prokaryotes have been shown to  
88 contribute to ~30% of the  $\text{NO}_3^-$  and  $\text{NH}_4^+$  community uptake rates (Kirchman and Wheeler 1998).  
89 Comparable contributions (~40%) were found in a eutrophic coastal Mediterranean lagoon (Trottet et  
90 al. 2011) and in Sub-Arctic Atlantic (Fouilland et al. 2007) while much smaller (4-14%) were observed  
91 in the post-bloom temperate waters of the North Atlantic (Kirchman et al. 1994). In parallel, an  
92 increasing number of studies show that photosynthetic organisms use Dissolved Organic N (DON)  
93 compounds for their growth (Bronk et al. 2007). For example, urea is thought to fuel the recurrent  
94 harmful algal blooms of *Aureococcus anophagefferens* (Berg et al. 1997). The ability of  
95 *Prochlorococcus* to use dissolved free amino acid has been hypothesized to explain its dominance in  
96 oligotrophic waters where inorganic N is depleted (Zubkov et al. 2003).

97 Despite the growing body of evidence for the prevalence of mixed nutritional strategies and the clear  
98 implications for N and C resource competition, few studies have simultaneously investigated the uptake  
99 of organic and inorganic N and C by pigmented and non-pigmented planktonic communities (Bradley  
100 et al. 2010). The lack of observations can in part be explained by the methodological challenge of  
101 measuring these processes *in situ* at the plankton group scale. The most common approach combines

102 stable or radioactive isotope labelling and post incubation size fractionation where large and small size  
103 fractions are attributed to photosynthetic groups and non-pigmented prokaryotes, respectively, with a  
104 typical cut-off at 0.7-1  $\mu\text{m}$  (Kellogg and Deming 2009; Schapira et al. 2012). However, retention of  
105 non-pigmented prokaryotes in the largest size fractions has been shown to be significant, in particular  
106 embedded in aggregates and/or attached to the cell surface of large organisms (Seymour et al. 2017).  
107 Similarly, the smallest pigmented groups, such as *Prochlorococcus* or *Ostreococcus*, are within the size  
108 spectrum of non-pigmented prokaryotes leading to an overall poor specificity of size fractionation,  
109 particularly in open ocean waters where small cells dominate photosynthetic communities (Casey et al.  
110 2019). Inhibitors specific to plankton groups have also been used to assess the contribution of  
111 prokaryotes to the uptake of inorganic nutrients (Fouilland et al. 2007). However, the efficiency and the  
112 specificity of the inhibitors in natural planktonic communities is questionable (Oremland and Capone  
113 1988). Flow cytometric cell sorting has been used in combination with radioactive isotope labelling  
114 allowing the determination of uptake rates of inorganic or organic substances labelled with  $^{14}\text{C}$ ,  $^{33}\text{P}$ ,  $^{35}\text{S}$   
115 or  $^3\text{H}$  at the group-level (e.g. Jardillier et al. 2010; Duhamel et al. 2019). Approaches using radioactive  
116 isotopes present the advantage of higher sensitivity than stable isotopes. They have been used to  
117 evidence group specific patterns such as the in-situ *Prochlorococcus* uptake of amino acids (Muñoz-  
118 Marín et al. 2020), the ingestion of non-pigmented prokaryotes cells by photosynthetic pico-eukaryotes  
119 (Hartmann et al. 2012; Duhamel et al. 2019) or the faster growth of *Prochlorococcus* and *Synechococcus*  
120 compared to photosynthetic pico-eukaryotes (Zubkov 2014). Unfortunately, there is no suitable  
121 radioactive tracer for N.

122 In this study, we circumvent these methodological issues by coupling dual stable isotope labelling assays  
123 ( $^{13}\text{C}$ ,  $^{15}\text{N}$ ) with flow cytometry cell sorting and nanoSIMS to measure at the single cell level the use of  
124 inorganic (dissolved inorganic C,  $\text{NH}_4^+$  and  $\text{NO}_3^-$ ) and organic (urea, leucine) sources of N and C by  
125 *Prochlorococcus*, *Synechococcus*, photosynthetic pico-eukaryotes and non-pigmented prokaryotes. We  
126 applied our approach in various biomes of the northwestern Atlantic, from the subtropical gyre to the  
127 Gulf Stream and Labrador Current. A common characteristic of these regions is a general state of  
128 nitrogen or phosphorus limitation (Wu et al. 2000; Lipschultz 2001; Moore et al. 2008). While

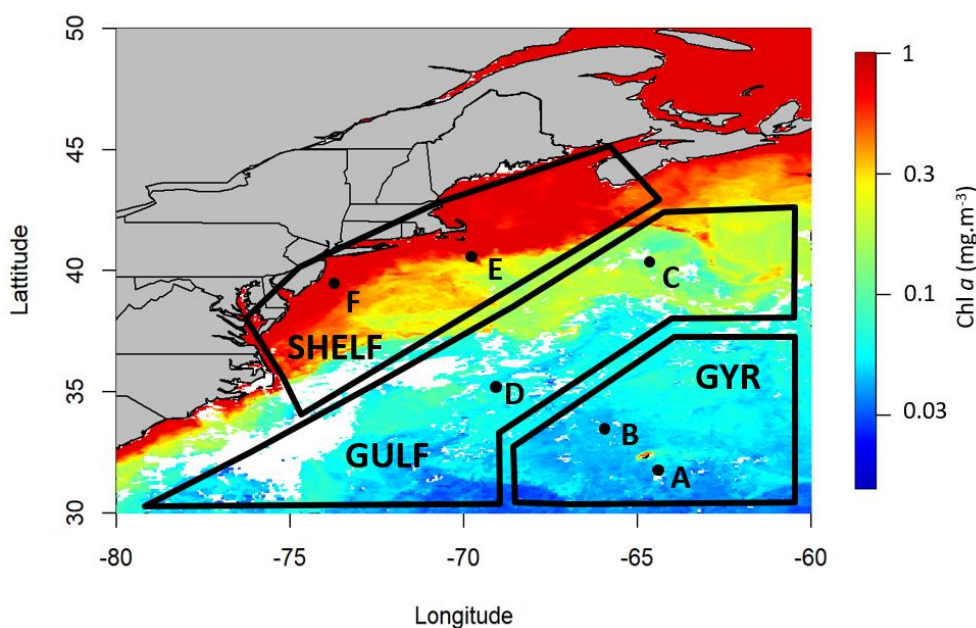
129 wintertime mixing can bring  $\text{NO}_3^-$  and phosphate ( $\text{PO}_4^{3-}$ ) rich waters to the surface (even in the  
130 oligotrophic waters near Bermuda), summer stratification leads to a reduction in nutrient availability in  
131 oceanic and coastal waters to levels limiting primary production as demonstrated by nutrient addition  
132 bioassays, in particular for N (Sedwick et al. 2018). This study provides a direct *in situ* comparison of  
133 N and C uptake by pigmented and non-pigmented picoplankton at the single cell level, highlighting the  
134 contrasting nutritional strategies sustaining the growth of specific picoplankton groups in the ocean.

## 135 **Materials**

### 136 *Sampling and biogeochemical analyses*

137 The study was conducted in the northwestern Atlantic between Bermuda and the United States New  
138 England coast aboard of the R/V *Atlantic Explorer* in August 2017. Six stations with contrasting  
139 biogeochemistry were sampled: two stations in the North Atlantic Gyre (stations A and B) among which  
140 one is the Bermuda Atlantic Time-series Study (BATS) station (hereafter Station A), two stations in the  
141 Gulf Stream (stations C and D) and two stations on the continental shelf of the coast of New England  
142 (stations E and F) (Fig. 1). Surface seawater samples (5 m) were collected using Niskin bottles mounted  
143 on a rosette equipped with CTD sensors. At each station, samples for dissolved N nutrients were  
144 collected in triplicate and filtered through combusted GF/F filters (4h, 450°C) before being stored at -  
145 20°C until further analysis. Care was taken to copiously rinse the filters with ultrapure water and  
146 seawater before sampling in order to avoid contaminations. Samples for  $\text{NO}_3^-$ , urea and  $\text{PO}_4^{3-}$  were  
147 collected in acid cleaned (soaked in hydrochloric acid 10%, followed by ultrapure water three times)  
148 polypropylene tubes (50 mL or 15 mL) and measured colorimetrically according to Raimbault et al.  
149 (1990), Mulvenna and Savidge (1992) and Strickland and Parsons (1972), respectively. The limits of  
150 detection were 10, 60 and 14  $\text{nmol N L}^{-1}$  for  $\text{NO}_3^-$ , urea and  $\text{PO}_4^{3-}$ , respectively. Samples for  $\text{NH}_4^+$  were  
151 collected in 50 mL polypropylene tubes which were conditioned beforehand to reduce risks of  
152 contamination: the tubes were first left overnight in hydrochloric acid 10%, rinsed three times with  
153 freshly produced ultrapure water and filled in a mixture of ultra-pure water and reagents for  $\text{NH}_4^+$   
154 determination until sampling. Samples were then measured fluorimetrically as described in Holmes et

155 al. (1999) with standards made from  $\text{NH}_4^+$ -free deep seawater stored in the same conditions as samples.  
156 The limit of detection was  $3 \text{ nmol N L}^{-1}$ .



157  
158 *Figure 1. Location of the stations and the oceanic regions sampled in the northwestern Atlantic Ocean*  
159 *(SHELF: continental shelf, GULF: Gulf Stream, GYR: North Atlantic Gyre) superimposed on surface*  
160 *chlorophyll a (Chl a) concentration (in  $\text{mg}\cdot\text{m}^{-3}$ ) from AQUA/MODIS (composite image of August*  
161 *2017).*

## 162 **Experimental design**

163 At each station, uptake of dissolved inorganic C (hereafter referred to as C-fixation),  $\text{NH}_4^+$ ,  $\text{NO}_3^-$ , urea  
164 and leucine were measured using stable isotope tracer incubations both at the plankton-community and  
165 at the single-cell levels. For this purpose, seawater was collected at each station from the Niskin bottles  
166 in four sets of five acid-cleaned 1.2 L polycarbonate bottles. Isotope-labelled tracers were added in all  
167 the bottles directly after collection as follow:  $^{13}\text{C}$  was added under the form of dissolved inorganic C  
168 ( $\text{NaH}^{13}\text{CO}_3$ , 99%, Eurisotop) together with either  $^{15}\text{NO}_3^-$  ( $\text{KNO}_3$ , 98%, Eurisotop),  $^{15}\text{NH}_4^+$  ( $\text{NH}_4\text{Cl}$ , 98%,  
169 Eurisotop) or  $^{15}\text{N}$ -urea (98%, Eurisotop) or under the form of dual-labeled  $^{13}\text{C}$ - $^{15}\text{N}$  leucine (99%  $^{13}\text{C}$  and  
170 98%  $^{15}\text{N}$ ). C-fixation rates were calculated from the average of incubations performed in the presence  
171 of  $^{15}\text{NO}_3^-$ ,  $^{15}\text{NH}_4^+$  and  $^{15}\text{N}$ -urea. Isotopes were added to a final concentration of  $30 \text{ nmol N L}^{-1}$  for  $\text{NH}_4^+$ ,  
172  $\text{NO}_3^-$  and urea at the gyres and at the Gulf Stream stations and  $50 \text{ nmol N L}^{-1}$  at the continental shelf



173 stations. Due to expected relatively low uptake rates, leucine was added at the saturating (or close to  
174 saturating) concentrations of 10 nmol L<sup>-1</sup> at all stations to ensure significant isotopic enrichments (Hill  
175 et al. 2013). In order to determine the initial <sup>13</sup>C and <sup>15</sup>N isotopic abundance in the particulate matter,  
176 one bottle from each set was filtered onto combusted GF/F (4 h, 450 °C) directly after the addition of  
177 the isotopes. Filters were rinsed with 0.2 µm pore-size filtered seawater and stored at -20 °C. The  
178 remaining bottles from the set were placed in an on-deck incubator reproducing the light intensity at the  
179 surface and kept at sea surface temperature by a continuous circulation of surface seawater. The  
180 incubations lasted 3–8 h (5.5 h on average), except for the leucine treatments for which incubations  
181 lasted 22–24 h in order to ensure significant isotopic enrichments. Incubations were stopped by filtering  
182 three of the four remaining bottles from each set onto combusted GF/F as described above. The last  
183 bottle from each set was used to concentrate the cells for flow cytometry cell sorting. For this purpose,  
184 the bottle content was filtered onto 0.2 µm polycarbonate filters. The filtration was stopped just before  
185 the filter went dry and ~10 mL of 0.2 µm filtered sea water with PFA (1.6% final concentration) was  
186 added on the filter and left for 1 h in the dark. The solution was then filtered, the filters were placed in  
187 5 mL cryotubes filled with 0.2 µm filtered seawater. The cryotubes were vortexed in order to resuspend  
188 the cells in the solution, then flash frozen in liquid N<sub>2</sub> and stored at -80°C.

### 189 *Flow cytometry cell sorting and isotopic analyses*

190 Flow cytometry cell sorting and nanoSIMS analyses were conducted as previously described in  
191 Berthelot et al. (2019) with a few modifications. Concentrated cells in cryotubes were sorted back  
192 onshore using a BD Influx cell sorter equipped with a 70 µm nozzle, with sheath fluid and sample fluid  
193 pressure of 30 PSI (207 kPa) and 31 PSI (214 kPa), respectively. The instrument was set at the highest  
194 sorting purity (1.0 drop single mode), the drop delay was calibrated using Accudrop Beads (BD  
195 Biosciences, USA) and the sorting efficiency was verified manually by sorting a specified number of 1  
196 µm yellow–green microspheres (Polysciences #17154-10) onto a glass slide and counting the beads  
197 under an epifluorescence microscope. We systematically recovered 100% of the targeted beads before  
198 sorting samples. Using this setup, the sorting purity on our instrument typically exceeds 96% (Duhamel  
199 et al. 2019). *Prochlorococcus*, *Synechococcus* and photosynthetic pico-eukaryotes were discriminated

200 in unstained samples while non-pigmented prokaryotes were discriminated in a sample aliquot stained  
 201 with SYBR Green I DNA dye (0.01% final). non-pigmented prokaryotes clustered in two groups: low  
 202 nucleic acid and high nucleic acid. Using a forward scatter detector with small particle option and  
 203 focusing a 488 plus a 457 nm (200 and 300 mW solid state respectively) laser into the same pinhole  
 204 allowed the resolution of dim surface *Prochlorococcus* population from background noise in unstained  
 205 samples. However, in stained samples, *Prochlorococcus* overlapped with high nucleic acid group and  
 206 therefore, only cells belonging to low nucleic acid group were sorted and further analyzed for isotopic  
 207  $^{13}\text{C}$  and  $^{15}\text{N}$  contents and are referred collectively as non-pigmented prokaryotes. Filters containing the  
 208 sorted cells were analyzed on a CAMECA nanoSIMS 50 using a focused 1.2 pA  $\text{Cs}^+$  ion beam scanning  
 209 fields of 10 x 10  $\mu\text{m}$  (for non-pigmented prokaryotes and *Prochlorococcus*), 20 x 20  $\mu\text{m}$  (for  
 210 *Synechococcus*) and 30 x 30  $\mu\text{m}$  (for photosynthetic pico-eukaryotes) and recording alternatively the  
 211  $^{12}\text{C}^{14}\text{N}^-$  and  $^{12}\text{C}^{15}\text{N}^-$  or  $^{12}\text{C}^{14}\text{N}^-$  and  $^{13}\text{C}^{14}\text{N}^-$  secondary ions using the “peak jumping mode” over at least  
 212 20 planes. Mass resolution was  $>7,000$  to resolve the  $^{12}\text{C}^{15}\text{N}^-$  and  $^{13}\text{C}^{14}\text{N}^-$  ions (See Berthelot et al. 2019  
 213 for further details). Cells were then identified based on the  $^{12}\text{C}^{14}\text{N}^-$  total ion count images and outlined  
 214 using the particle detection mode of the LIMAGE software. Each particle detected was individually  
 215 checked and redrawn if needed or discarded when it was not possible to attribute it to a cell with  
 216 certainty. Particulate C and N concentrations and isotopic ratios at the community scale were determined  
 217 on an isotope ratio mass spectrometer coupled to an elemental analyzer (EA-IRMS) from the triplicate  
 218 GF/F filters. At the average C and N content measured on the samples ( $\sim 6 \mu\text{mol C}$  and  $\sim 0.9 \mu\text{mol N}$ ),  
 219 the precision (standard deviation of repeated measurements) of the elemental analyses were  $0.08 \mu\text{mol}$   
 220 C and  $0.007 \mu\text{mol N}$  and the precision of the isotopic percent abundances were  $0.0004 \text{ atom\%}$  and  
 221  $0.0003 \text{ atom\%}$  for C and N, respectively.

## 222 ***Rate calculations and statistical analyses***

223 For each cell analyzed, the isotopic percent abundances of  $^{13}\text{C}$  ( $A^{13}\text{C} = \frac{^{13}\text{C}^{14}\text{N}^-}{^{13}\text{C}^{14}\text{N}^- + ^{12}\text{C}^{14}\text{N}^-} * 100$ ) and  $^{15}\text{N}$   
 224 ( $A^{15}\text{N} = \frac{^{12}\text{C}^{15}\text{N}^-}{^{12}\text{C}^{14}\text{N}^- + ^{12}\text{C}^{15}\text{N}^-} * 100$ ) were used to calculate the element (C- or N-) specific uptake rate (h<sup>-1</sup>):  
 225

226 
$$\text{element specific uptake} = \frac{A_{\text{cell}} - \bar{A}_{t0}}{A_{\text{source}} - \bar{A}_{t0}} * \frac{1}{t}$$

227 where  $A_{\text{cell}}$ ,  $\bar{A}_{t0}$ , and  $A_{\text{source}}$  are the isotopic percent abundances of the cell after incubation ( $A_{13C}$  or  
 228  $A_{15N}$ ), of the cells (mean) prior to incubation, and of the source pool, respectively and  $t$  is the incubation  
 229 time. Note that in the case of dissolved inorganic C, the specific uptake rates are termed C-specific C-  
 230 fixation rate. In addition to C- and N-specific uptake rates, C-fixation based division rates were  
 231 calculated as follows:

232 
$$\text{C fixation based division} = \log_2 \left( \frac{A_{\text{source}} - \bar{A}_{t0}}{A_{\text{source}} - A_{\text{cell}}} \right) * \frac{1}{t}$$

233 C-fixation based division rates reflect cellular division rates if inorganic C-fixation is the unique source  
 234 of elemental C to the organism, as would be the case in case of exclusive photoautotrophy. For  
 235 comparison with the literature, C-fixation division rates are presented in  $d^{-1}$ . As the incubations were not  
 236 performed from dawn to dusk, hourly rates were converted to daily rates using the model developed by  
 237 Moutin et al. (1999) which account for the variation of daylight intensity at the sampling site and on the  
 238 sampling day.

239 Cell-specific uptake rates ( $\text{amol C cell}^{-1} \text{ h}^{-1}$  and  $\text{amol N cell}^{-1} \text{ h}^{-1}$ ) were calculated as follows:

240 
$$\text{cell specific uptake} = \frac{A_{\text{cell}} - \bar{A}_{t0}}{A_{\text{source}} - \bar{A}_{t0}} * \frac{1}{t} * Q_{\text{cell}}$$

241 With  $Q_{\text{cell}}$  the estimated C and N cell contents. For pigmented organisms, C and N cell contents used  
 242 were the median values reported by Baer et al. (2017) in northwestern Atlantic (5, 23 and 257  $\text{fmol C}$   
 243  $\text{cell}^{-1}$  and 0.6, 2.4 and 15  $\text{fmol N cell}^{-1}$  for *Prochlorococcus*, *Synechococcus* and photosynthetic pico-  
 244 eukaryotes, respectively). For non-pigmented prokaryotes, a C cell content of 1.7  $\text{fmol C cell}^{-1}$  and a  
 245 C:N ratio of 6.6 were used (Fukuda et al. 1998). The cell-specific uptake rates of dissolved inorganic C  
 246 are termed cell-specific C-fixation rates. Group uptake rates were obtained by multiplying per-cell rates  
 247 by cell abundances in the respective group.

248 Single cell uptake was considered to be above the detection limit when the percent abundance  
249 enrichment ( $A_{cell} - \bar{A}_{t0}$ ) was higher than two times the standard deviation associated with the Poisson  
250 distribution ( $\lambda$ ) parameterized as  $\lambda = A_{cell} * N_{CN^-,cell}$ , where  $N_{CN^-,cell}$  is the  $CN^-$  ions counts of the cell.  
251 Similarly, groups were considered as active when the mean cellular percent isotopic abundances  
252 enrichment of the groups ( $\bar{A}_{group} - \bar{A}_{t0}$ ) were two times higher than the standard deviation of the  
253 cellular percent abundances. Differences in C or N specific uptake between stations or groups were  
254 tested using unpaired Kruskal-Wallis test and considered significant if  $p < 0.05$ .

255 The community C and N uptake rates ( $nmol\ C\ L^{-1}\ h^{-1}$  or  $nmol\ N\ L^{-1}\ h^{-1}$ ) were measured from GF/F filters  
256 as follows:

$$257 \quad Community\ uptake = \frac{A_{PM} - \bar{A}_{t0}}{A_{source} - \bar{A}_{t0}} * \frac{1}{t} * PM$$

258 With PM the particulate C or N concentration and  $A_{PM}$  the isotopic percent abundance of  $^{13}C$  or  $^{15}N$  in  
259 the particulate matter.

260 Due to the low concentrations of  $NH_4^+$ ,  $NO_3^-$  and urea, isotopes tracers additions exceeded the threshold  
261 of 10% of the ambient concentrations for trace level additions. As a result, percent isotopic abundances  
262 in the source pool ( $A_{source}$ ) ranged between 41-95%. Two uptake kinetics experiments with increasing  
263 nutrient additions at the gyre stations were performed to assess the extent of overestimation of the uptake  
264 due to the  $^{15}N$  added. Rates were then corrected for this overestimation according to Harrison et al.  
265 (1996) to approximate *in situ* rates as much as possible. This correction resulted in a reduction of  $NH_4^+$ ,  
266  $NO_3^-$  and urea uptake rates by a factor 1.5, 2.4 and 1.1 on average, respectively. At stations where  $NO_3^-$   
267 was below the detection limit, we assumed a  $NO_3^-$  concentration of  $5\ nmol\ L^{-1}$  for the calculations.  
268 Leucine concentrations were not measured but assumed to be lower than  $1\ nmol\ L^{-1}$  (Zubkov et al. 2008)  
269 and uptake rates were calculated assuming percent isotopic abundances of  $^{13}C$  and  $^{15}N$  of 95% in the  
270 source pool. Leucine rates were not corrected from overestimation due to leucine addition at saturating  
271 (or close to saturating) concentrations and should thus be interpreted as “potential” rates. We did not  
272 correct for isotope dilution associated with regeneration of  $NH_4^+$  during the incubations, which would

273 tend to bias our estimates low. In order to limit this bias, the duration of the  $\text{NH}_4^+$  incubations were kept  
274 short ( $\leq 3.5$  h). Minimum quantifiable rates were calculated at each station and for each tracer from the  
275 propagation of errors of the different parameters involved in the community uptake rate calculations  
276 according to Gradoville et al. (2017) (Table S1). All community uptake rates were higher than the  
277 minimum quantifiable rates. Maximal N fluxes constrained by diffusion-limited N supply to single cells  
278 were calculated from the analytical solutions of diffusion to a sphere:

$$279 \quad \rho_{max} = 4\pi D r_0 (C_\infty - C_0)$$

280 where  $\rho_{max}$  is the maximal  $\text{NH}_4^+$ ,  $\text{NO}_3^-$  or urea uptake rate ( $\text{nmol s}^{-1}$ ) of a cell with the equivalent  
281 spherical radius  $r_0$  (cm),  $D$  is the diffusion coefficient ( $\text{cm}^2 \text{s}^{-1}$ ) of the considered compound in water,  
282  $C_0$  is the  $\text{NH}_4^+$  concentration at the cell surface (assumed to be zero) and  $C_\infty$  is the measured  
283 concentration in the ambient water. We assume diffusion coefficients of  $1.98 \times 10^{-5}$ ,  $1.90 \times 10^{-5}$  and  $1.38$   
284  $\times 10^{-5} \text{ cm}^2 \text{ s}^{-1}$  at  $25^\circ\text{C}$  for  $\text{NH}_4^+$ ,  $\text{NO}_3^-$  and urea, respectively (Longworth 1963; Li and Gregory 1974).

## 285 **Results**

### 286 *Biogeochemistry of the studied area*

287 The biogeochemical characteristics of the sampled stations are presented in Table 1. At the time of  
288 sampling, surface  $\text{NO}_3^-$ ,  $\text{NH}_4^+$  and urea concentrations were low:  $\text{NO}_3^-$  was below the detection limit (10  
289  $\text{nmol L}^{-1}$ ) and  $\text{NH}_4^+$  and urea concentrations ranged between 11–28  $\text{nmol N L}^{-1}$  and 91–173  $\text{nmol N L}^{-1}$ ,  
290 respectively, without clear patterns between regions. In contrast,  $\text{PO}_4^{3-}$  concentrations showed a strong  
291 pattern with higher concentrations at the continental shelf stations (110–152  $\text{nmol L}^{-1}$ ) than at the Gulf  
292 Stream (40–45  $\text{nmol L}^{-1}$ ) and the gyre (15–18  $\text{nmol L}^{-1}$ ) stations. In the surface waters of the gyre,  
293 Particulate C concentrations were  $\sim 2 \mu\text{mol C L}^{-1}$ . Particulate C concentrations were higher at the Gulf  
294 Stream stations (3–4  $\mu\text{mol C L}^{-1}$ ) and at the continental shelf stations (8–12  $\mu\text{mol C L}^{-1}$ ).

295 Table 1. Biogeochemistry of the six stations investigated. All the samples were collected in triplicates  
 296 (average  $\pm$  standard deviation), unless otherwise stated. ND: not detected.  
 297

Station	Temperature (°C)	Particulate C ( $\mu\text{mol C L}^{-1}$ )	Concentrations ( $\text{nmol N L}^{-1}$ or $\text{nmol P L}^{-1}$ )				Abundances ( $10^3 \text{ cell mL}^{-1}$ )				Community uptake rates ( $\text{nmol C L}^{-1} \text{ h}^{-1}$ or $\text{nmol N L}^{-1} \text{ h}^{-1}$ )					
			Nitrate	Ammonium	Urea	Phosphate	Non-pigmented prokaryotes	<i>Prochlorococcus</i>	<i>Synechococcus</i>	Photosynthetic pico-eukaryotes	C-fixation	Nitrate uptake	Ammonium uptake	Urea uptake	C-leucine potential uptake	N-leucine potential uptake
<b>North Atlantic Gyre</b>																
A	27.8	2.0 $\pm$ 0.2	<10	15 $\pm$ 1	92 $\pm$ 54	15 $\pm$ 3*	243 $\pm$ 10	11.0 $\pm$ 0.9	9.7 $\pm$ 1.7	0.5 $\pm$ 0.1	18.7 $\pm$ 2.8	0.4 $\pm$ 0.1	1.0 $\pm$ 0.4	1.0 $\pm$ 0.5	0.2 $\pm$ 0.0	0.1 $\pm$ 0.0
B	27.8	1.9 $\pm$ 0.2	<10	11 $\pm$ 2	173 $\pm$ 7	18 $\pm$ 4*	252 $\pm$ 19	12.2 $\pm$ 0.7	8.2 $\pm$ 0.9	0.4 $\pm$ 0.0	20.2 $\pm$ 2.0	0.4 $\pm$ 0.1	1.7 $\pm$ 0.3	1.8 $\pm$ 0.2	0.2 $\pm$ 0.1	0.1 $\pm$ 0.1
<b>Gulf Stream</b>																
C	26	4.0 $\pm$ 0.2	<10	11 $\pm$ 5	163 $\pm$ 47	40 $\pm$ 2*	584 $\pm$ 15	207.6 $\pm$ 18.0	26.8 $\pm$ 3.0	1.6 $\pm$ 0.4	66.7 $\pm$ 3.3	0.9 $\pm$ 0.0	3.0 $\pm$ 0.2	6.3 $\pm$ 0.7	0.4 $\pm$ 0.1	0.1 $\pm$ 0.1
D	23.3	3.5 $\pm$ 0.2	<10	18 $\pm$ 7	91 $\pm$ 14	45 $\pm$ 4*	381 $\pm$ 18	38.2 $\pm$ 5.8	57.7 $\pm$ 2.8	1.7 $\pm$ 0.2	64.6 $\pm$ 4.1	1.4 $\pm$ 0.6	4.8 $\pm$ 1.5	7.0 $\pm$ 1.8	0.5 $\pm$ 0.1	0.2 $\pm$ 0.1
<b>Continental Shelf</b>																
E	16.8	11.7 $\pm$ 1.5	<10	17 $\pm$ 0	144 $\pm$ 33	152 $\pm$ 4*	609 $\pm$ 65	ND	53.7 $\pm$ 5.4	12.2 $\pm$ 2.1	162.0 $\pm$ 7.8	3.8 $\pm$ 1.1	6.1 $\pm$ 0.8	9.8 $\pm$ 3.3	0.8 $\pm$ 0.3	0.3 $\pm$ 0.2
F	18.8	8.3 $\pm$ 1.8	<10	28 $\pm$ 7	106 $\pm$ 7	110 $\pm$ 2*	297 $\pm$ 12	ND	26.6 $\pm$ 1.9	4.7 $\pm$ 1.0	121.6 $\pm$ 19.7	3.7 $\pm$ 0.4	23.6 $\pm$ 5.0	11.0 $\pm$ 2.9	0.7 $\pm$ 0.1	0.3 $\pm$ 0.1

298 \* Duplicate samples.

299 The cyanobacteria *Prochlorococcus* and *Synechococcus* dominated the surface pigmented pico-plankton  
 300 community in the gyre with abundances in the same order of magnitude ( $\sim 10^4 \text{ cell mL}^{-1}$ ), while  
 301 photosynthetic pico-eukaryotes abundances were consistently lower than  $5 \cdot 10^2 \text{ cell mL}^{-1}$  (Table 1). In  
 302 the Gulf Stream, abundances were three times higher for photosynthetic pico-eukaryotes, three-to-seven  
 303 times higher for *Synechococcus* and four-to-ten times higher for *Prochlorococcus* (which reached  
 304 particularly high abundances at station C,  $> 2 \cdot 10^5 \text{ cell mL}^{-1}$ ) than in the gyre. At the continental shelf  
 305 stations, *Prochlorococcus* was not detected, while *Synechococcus* abundances were in the range of those  
 306 measured in the Gulf Stream and photosynthetic pico-eukaryotes were more abundant than in the two  
 307 other regions studied. Non-pigmented prokaryotes abundances ranged between  $2 \cdot 10^5$  to  $6 \cdot 10^5 \text{ cells mL}^{-1}$   
 308 with the lowest abundances observed in the gyre. Among non-pigmented prokaryotes, two-subgroups  
 309 were observed, characterized by their level of green fluorescence, which reflects their nucleic acid  
 310 content: low nucleic acid content and high nucleic acid content. Low nucleic acid sub-group numerically  
 311 dominated the non-pigmented prokaryotes group at the gyre stations (59–63%) in contrast to the Gulf  
 312 Stream and continental shelf stations (22–44%) (Table S2).

313 Community C-fixation in surface increased from the gyre ( $< 20 \text{ nmol C L}^{-1} \text{ h}^{-1}$ ) to the Gulf Stream ( $\sim 60$   
 314  $\text{nmol C L}^{-1} \text{ h}^{-1}$ ) and to the continental shelf ( $> 120 \text{ nmol C L}^{-1} \text{ h}^{-1}$ ) (Table 1). Similarly, community  $\text{NO}_3^-$   
 315 uptake rates were  $0.4 \text{ nmol N L}^{-1} \text{ h}^{-1}$  in the GYR,  $0.9\text{--}1.4 \text{ nmol N L}^{-1} \text{ h}^{-1}$  in the Gulf Stream and reached  
 316 as much as  $3.8 \text{ nmol N L}^{-1} \text{ h}^{-1}$  at the continental shelf stations. Community  $\text{NH}_4^+$  and N-urea uptake rates

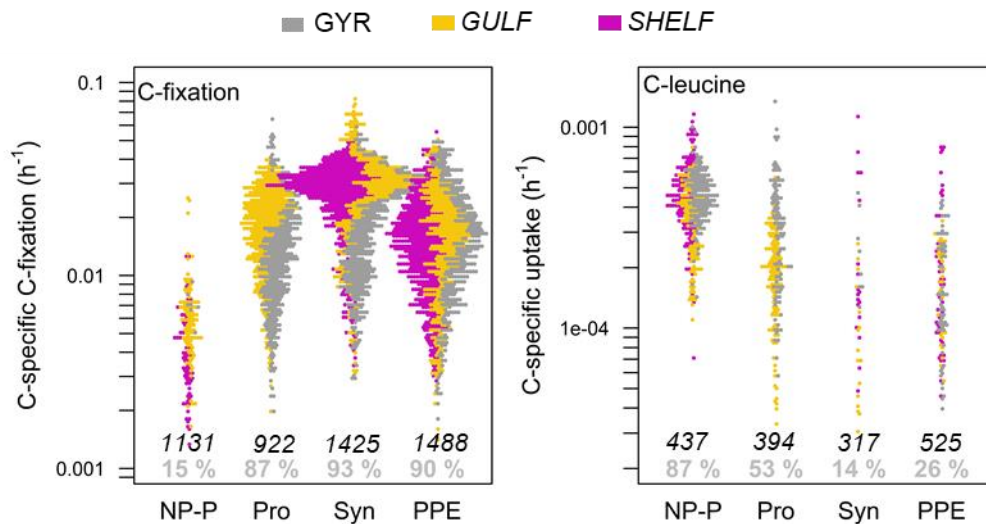
317 were within the same range at each region ( $<1.8$ ,  $3.0\text{--}7.0$  and  $6.1\text{--}23.6$   $\text{nmol N L}^{-1} \text{h}^{-1}$ , at the gyre, Gulf  
318 Stream and continental shelf stations, respectively). Community C- and N-leucine potential uptakes  
319 rates were low in comparison to the other N compounds investigated ( $0.2\text{--}0.8$   $\text{nmol C L}^{-1} \text{h}^{-1}$  and  $0.1\text{--}$   
320  $0.3$   $\text{nmol N L}^{-1} \text{h}^{-1}$ , respectively) but followed the same regional trends with higher rates on the  
321 continental shelf than in the Gulf Stream and gyre.

### 322 *Single cell metabolic rates of the cytometrically sorted groups*

323 Single cell analyses of cytometrically sorted groups allowed the determination of the cellular fixation or  
324 uptake rates of the  $^{13}\text{C}$  or  $^{15}\text{N}$  labelled substrates tested (Fig. 2, 3 and Table S3). The results are presented  
325 in C- and N-specific uptake rates ( $\text{h}^{-1}$ ) to allow for the comparison of metabolic activities between cells  
326 with different biomass content. Cell-specific uptake rates ( $\text{amol C cell}^{-1} \text{h}^{-1}$  and  $\text{amol N cell}^{-1} \text{h}^{-1}$ ) and C-  
327 fixation based division rates ( $\text{d}^{-1}$ ) are also presented in Table S3, S4 and Fig. S1 for comparison with  
328 literature data. Intragroup C-specific C-fixation rates varied greatly, from undetectable to more than  $0.1$   
329  $\text{h}^{-1}$  (Fig. 2). However, when averaged, clear patterns appeared between the different groups sorted and  
330 between regions. C-specific C-fixation was detected for a subset of the non-pigmented prokaryotes cells  
331 (15% on average) but at the group scale significant activities were not detected at any stations (see  
332 criteria in the experimental procedure section). In contrast, significant C-specific C-fixation was always  
333 detected for pigmented groups (averaging  $0.016\pm 0.010$ ,  $0.022\pm 0.015$  and  $0.016\pm 0.012$   $\text{h}^{-1}$  for  
334 *Prochlorococcus*, *Synechococcus* and photosynthetic pico-eukaryotes, respectively). C-specific C-  
335 fixation rate was on average twice higher in the Gulf Stream than in the gyre for *Prochlorococcus*.  
336 Similarly, *Synechococcus* displayed higher activity in the Gulf Stream and the continental shelf as  
337 compared to the gyre. In contrast, no clear trends were observed between regions for photosynthetic  
338 pico-eukaryotes.

339 When detected, C-specific leucine potential uptake rates were higher on average in non-pigmented  
340 prokaryotes ( $0.0004\pm 0.0002$   $\text{h}^{-1}$  on average) than in pigmented organisms ( $0.0001\pm 0.0001$   $\text{h}^{-1}$  on  
341 average). Among the pigmented groups, *Prochlorococcus* showed the highest C-specific leucine  
342 potential uptake rates and the highest proportion of active cells ( $0.0002\pm 0.0055$   $\text{h}^{-1}$ , 53% of active cells),

343 as compared to photosynthetic pico-eukaryotes ( $0.0001 \pm 0.0001 \text{ h}^{-1}$ , 26% of active cells) and  
 344 *Synechococcus* ( $< 0.0001 \text{ h}^{-1}$ , 14% of active cells), respectively, and no clear patterns were observed  
 345 between regions (Fig. 2).



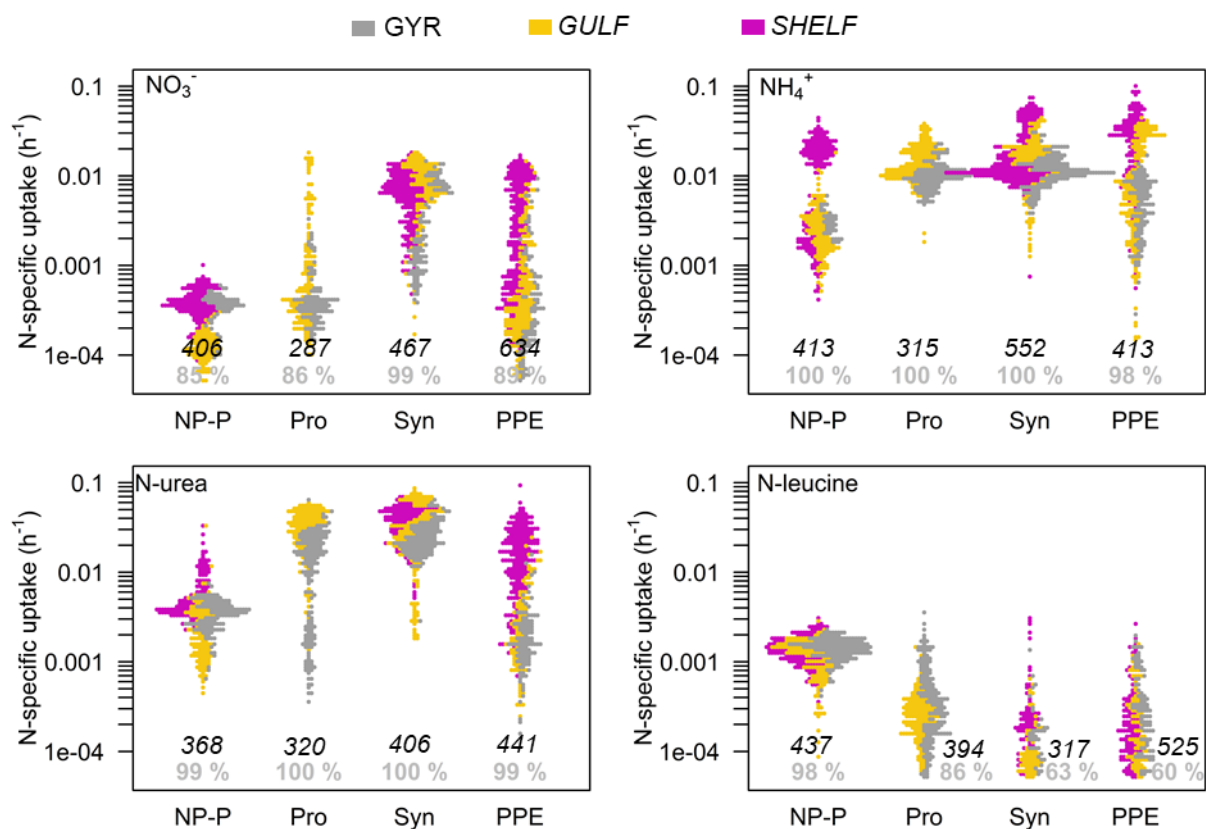
346

347 *Figure 2. Single cell C-specific C-fixation rates and C-specific leucine potential uptake rates ( $\text{h}^{-1}$ ) for*  
 348 *each group investigated (NP-P: non-pigmented prokaryotes, Pro: Prochlorococcus, Syn:*  
 349 *Synechococcus, PPE: photosynthetic pico-eukaryotes). Each point represents an analyzed cell. Only*  
 350 *the cells with detected activity with respect to the process under study are shown. Italic black numbers*  
 351 *denote the number of cells analyzed for each group. Grey numbers denote the proportion (in %) of*  
 352 *cells for which activity was detected. Colors denote the sampling regions (North Atlantic Gyre (GYR),*  
 353 *Gulf Stream (GULF) and continental shelf (SHELF) in grey, yellow and purple, respectively). Note the*  
 354 *order of magnitude difference between the two-logarithm y-scales.*

355 N-specific uptake rates were also highly variable between cells (Fig. 3). In the gyre and Gulf Stream  
 356 regions where all three groups were detected, N-specific  $\text{NH}_4^+$  uptake rate was on average slightly higher  
 357 for *Synechococcus* ( $0.014 \pm 0.008 \text{ h}^{-1}$ ) than for *Prochlorococcus* ( $0.013 \pm 0.006 \text{ h}^{-1}$ ) and photosynthetic  
 358 pico-eukaryotes ( $0.010 \pm 0.010 \text{ h}^{-1}$ ) and higher for pigmented groups ( $0.012 \pm 0.004 \text{ h}^{-1}$ ) than for non-  
 359 pigmented prokaryotes ( $0.003 \pm 0.006 \text{ h}^{-1}$ ) (each group was significantly different from each other,  
 360  $p < 0.05$ ). N-specific urea uptake was the highest on average for *Synechococcus* ( $0.030 \pm 0.018 \text{ h}^{-1}$ )  
 361 followed by *Prochlorococcus* ( $0.023 \pm 0.016 \text{ h}^{-1}$ ), photosynthetic pico-eukaryotes ( $0.003 \pm 0.004 \text{ h}^{-1}$ ) and  
 362 non-pigmented prokaryotes ( $0.003 \pm 0.002 \text{ h}^{-1}$ ), respectively (each group were significantly different



363 from each other,  $p < 0.05$ ). N-specific  $\text{NO}_3^-$  uptake rates were on average higher for *Synechococcus*  
 364 ( $0.006 \pm 0.005 \text{ h}^{-1}$ ) compared to photosynthetic pico-eukaryotes ( $0.001 \pm 0.002 \text{ h}^{-1}$ ), *Prochlorococcus*  
 365 ( $0.001 \pm 0.003 \text{ h}^{-1}$ ) and non-pigmented prokaryotes ( $< 0.001 \text{ h}^{-1}$ ), respectively (each group were  
 366 significantly different from each other,  $p < 0.05$ ). Noticeably, at station C *Prochlorococcus* N-specific  
 367  $\text{NO}_3^-$  uptake peaked at  $0.004 \pm 0.005 \text{ h}^{-1}$ , a rate much higher than the one observed in photosynthetic pico-  
 368 eukaryotes ( $0.002 \pm 0.003 \text{ h}^{-1}$ ). N-specific leucine potential uptake was an order of magnitude lower  
 369 compared to the three other N substrates studied and was highest for non-pigmented prokaryotes  
 370 ( $0.0013 \pm 0.0005 \text{ h}^{-1}$ ) as compared to the phytoplankton groups studied ( $0.0004 \pm 0.0004 \text{ h}^{-1}$ ,  
 371  $0.0001 \pm 0.0001 \text{ h}^{-1}$ ,  $0.0002 \pm 0.0003 \text{ h}^{-1}$  for *Prochlorococcus*, *Synechococcus* and photosynthetic pico-  
 372 eukaryotes, respectively).



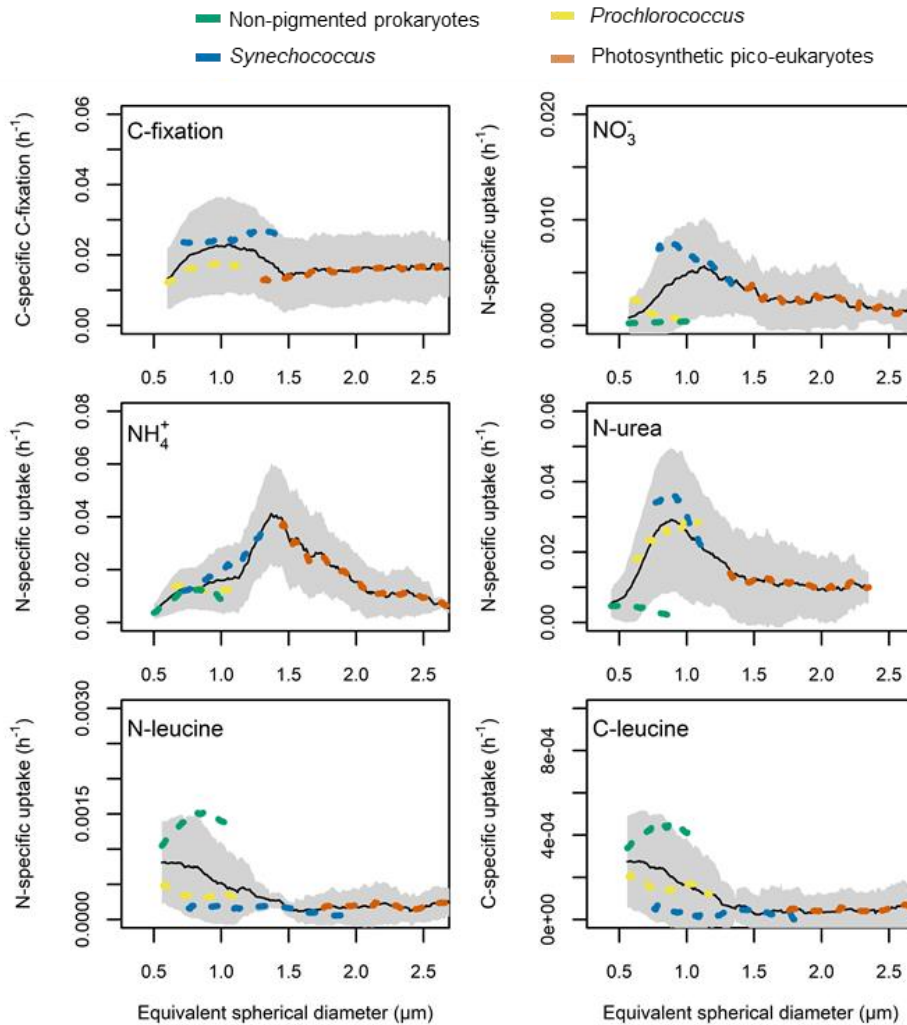
373  
 374 *Figure 3. Single cell N-specific nitrate ( $\text{NO}_3^-$ ), ammonium ( $\text{NH}_4^+$ ), urea and leucine specific uptake*  
 375 *rates ( $\text{h}^{-1}$ ) for each group (NP-P: non-pigmented prokaryotes, Pro: Prochlorococcus, Syn:*  
 376 *Synechococcus, PPE: photosynthetic pico-eukaryotes). Each point represents an analyzed cell. Only*  
 377 *the cells with detected activity with respect to the process under study are shown. Italic black numbers*  
 378 *denote the number of cells analyzed for each group. Grey numbers denote the proportion (in %) of*

379 cells for which activity was detected. Colors denote the sampling regions (North Atlantic Gyre (GYR),  
380 Gulf Stream (GULF) and continental shelf (SHELF) in grey, yellow and purple, respectively).

381 At the intra group scale, the C-specific C-fixation uptake rates were relatively stable as a function of cell  
382 size. However, the higher C-specific C-fixation rate of *Synechococcus* lead to a peak of rates centered  
383 around 1  $\mu\text{m}$  in equivalent spherical diameter when all the groups are considered together (Fig. 4). Cell  
384 size rates dependent patterns appeared more clearly at the intragroup levels for the other parameters  
385 measured. Intriguingly, the N-specific uptake rates seemed to be more influenced by cell size rather than  
386 group identity. For  $\text{NH}_4^+$ ,  $\text{NO}_3^-$  and N-urea patterns were similar with rates peaking for cells of size ca  
387 1.5, 1.2 and 1.0  $\mu\text{m}$  equivalent spherical diameter, respectively. For C- and N-specific leucine potential  
388 uptake rates, no peaks were observed but a decrease with increasing cell size.

389

390

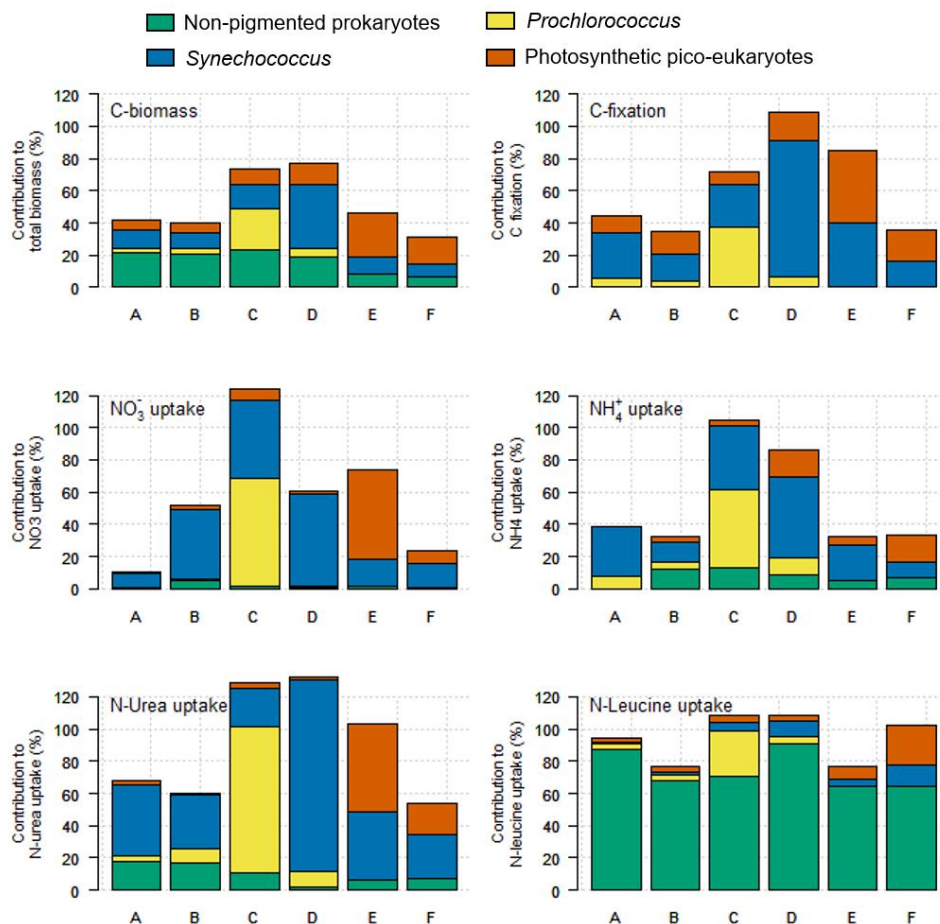


391  
 392 *Figure 4. Single cell C- and N-specific C-fixation, nitrate (NO<sub>3</sub><sup>-</sup>), ammonium (NH<sub>4</sub><sup>+</sup>), urea and leucine*  
 393 *uptake rates (h<sup>-1</sup>) as a function of cell size. The black lines and the shaded area denote the average and*  
 394 *standard deviation of rates for all the groups analyzed (except non-pigmented prokaryotes in the case*  
 395 *of C-fixation). Colored dashed lines denote group specific uptake rates (non-pigmented prokaryotes,*  
 396 *Prochlorococcus, Synechococcus and photosynthetic pico-eukaryotes in green, yellow, blue and red,*  
 397 *respectively).*

398 Using C and N cell contents estimated from the literature and measured abundances, we computed  
 399 groups' absolute rates and compared them to the community rates measured on the GF/F filters (Fig. 5).  
 400 Pico-plankton (sum of non-pigmented prokaryotes, *Prochlorococcus*, *Synechococcus* and  
 401 photosynthetic pico-eukaryotes) represented a significant fraction of the community C biomass  
 402 (52±17% on average) and of the community C-fixation (63±27% on average) with large variability

403 between stations (ranging from 35% to more than 100% of the community C-fixation). The contribution  
 404 of groups to the community N species uptake was also noticeably variable between stations. For  
 405 example, *Prochlorococcus* and photosynthetic pico-eukaryotes explained less than 10% of the  
 406 community  $\text{NO}_3^-$  uptake, except at stations C and E, where these groups contributed to more than 55%  
 407 of the community  $\text{NO}_3^-$  uptake. Similar patterns were also observed for  $\text{NH}_4^+$  and N-urea uptake at these  
 408 stations, which were explained by a conjunction of high abundances and high N-specific uptake. On  
 409 average, the sum of pico-sized pigmented groups accounted for a relatively large fraction of  $\text{NH}_4^+$  uptake  
 410 ( $47 \pm 27\%$ ),  $\text{NO}_3^-$  uptake ( $62 \pm 49\%$ ) and N-urea uptake ( $80 \pm 35\%$ ). The contribution of non-pigmented  
 411 prokaryotes to N uptake were much lower (averaging  $7 \pm 3\%$ ,  $2 \pm 2\%$  and  $9 \pm 5\%$  for  $\text{NH}_4^+$ ,  $\text{NO}_3^-$  and N-  
 412 urea, respectively). In contrast, this group was the main contributor to the community N-leucine  
 413 potential uptake (range 42-54%).

414



415

416 *Figure 5. Contribution of picoplankton groups to the community C-biomass, C-fixation, nitrate (NO<sub>3</sub><sup>-</sup>),*  
417 *ammonium (NH<sub>4</sub><sup>+</sup>), N-urea and N-leucine uptake rates at each station investigated. Colors denote the*  
418 *analyzed groups (non-pigmented prokaryotes, Prochlorococcus, Synechococcus and photosynthetic*  
419 *pico-eukaryotes in green, yellow, blue and red, respectively).*

## 420 **Discussion**

### 421 *Methodological considerations*

422 The role of various groups of pico-plankton in ocean C and N cycling remains poorly resolved in part  
423 because of a lack of appropriate methodological tools. Since the first applications to environmental  
424 microbiology more than a decade ago, nanoSIMS coupled to isotope labelling assays has gained in  
425 popularity and has been used to measure the contribution of different microbial groups to the community  
426 activity (Klawonn et al. 2016; Berthelot et al. 2019). Using this approach, we show in this study that  
427 picoplankton account for more than half of the community C-fixation in our study region (63% on  
428 average). This result is in line with previous measurements made in this area, and more generally in  
429 oligotrophic environments, using <sup>14</sup>C-sodium bicarbonate radioassays coupled with size fractionation or  
430 cell sorting (Jardillier et al. 2010; Duhamel et al. 2019). It is important to note that the cell-specific and  
431 group-specific uptake rates derived from nanoSIMS approaches rely on cell content data independently  
432 measured or reported in the literature which can vary by up to an order of magnitude between studies  
433 (Martiny et al. 2013; Baer et al. 2017). In our study, we used biomass cell contents measured from  
434 samples obtained in our sampling area, the northwestern Atlantic ocean (Baer et al. 2017). The derived  
435 cell-specific C-fixation rates (51–102, 317–806 and 2872–5388 amol C h<sup>-1</sup> for *Prochlorococcus*,  
436 *Synechococcus* and photosynthetic pico-eukaryotes, respectively) are in good agreement with values  
437 recently reported in the literature (Jardillier et al. 2010; Zubkov 2014; Duhamel et al. 2019)(Fig. S1).  
438 These cell contents carry uncertainty (coefficient of variation of ±30% to >100%) which can affect the  
439 cell and group specific uptake rates to the same extent and may bias the estimated contribution of groups  
440 to the community uptake (Fig. 5). The estimated contribution of small cells measured here could also  
441 be biased by active cells passing through GF/F filters (Bombar et al. 2018). This would lead to an  
442 underestimation of the community rates and could explain the picoplankton rates being higher than

443 community rates at some stations (Fig. 5). Using the cells outlined from nanoSIMS images, we measured  
444 that 54% of the non-pigmented prokaryotes, 31% of the *Prochlorococcus* and 7% of the *Synechococcus*  
445 cells had an equivalent spherical diameter lower than the 0.7  $\mu\text{m}$  nominal porosity of GF/F filters (Fig.  
446 S2) which is in line with previous reports showing that up to ~50% of the non-pigmented prokaryotes  
447 and <10% of the cyanobacteria cells eventually pass through GF/F filters (Lee et al. 1995; Morán et al.  
448 1999; Bombar et al. 2018). The combustion of GF/F filters might decrease the nominal pore size (Nayar  
449 and Chou 2003). In the future, the use of silver filters with a pore size of 0.2  $\mu\text{m}$  or the Advantex glass  
450 fiber filters with a nominal pore size of 0.3  $\mu\text{m}$  (both compatible with elemental analyzers) could reduce  
451 the number of cells passing through the filters (Bombar et al. 2018).

452 Based on the relatively low leucine uptake rates in the open ocean (Zubkov et al. 2008), we added leucine  
453 at saturating (or close to saturating) concentrations of 10  $\text{nmol L}^{-1}$  in order to ensure significant isotopic  
454 signal in our samples. The rates provided thus reflect “potential” rates rather than absolute rates. The  
455 leucine community uptake rates measured here (0.1-0.3  $\text{nmol leucine L}^{-1} \text{h}^{-1}$ ) are at the higher end of  
456 those reported using trace levels isotopes additions (i.e. additions of leucine < 0.5  $\text{nmol L}^{-1}$ ) in N.  
457 Atlantic with the more sensitive radiotracer assays (~0.01-0.1  $\text{nmol leucine L}^{-1} \text{h}^{-1}$ ) (Zubkov et al. 2003;  
458 Mary et al. 2008; Hill et al. 2013). Addition of leucine at saturating concentration (20  $\text{nmol L}^{-1}$ ) in the  
459 N. Atlantic resulted in a doubling of leucine uptake rates as compared to those obtain from trace level  
460 additions (0.4  $\text{nmol L}^{-1}$ ) (Hill et al. 2013). This provides some insight into the extent of the rate  
461 overestimation presented in our study.

#### 462 ***Could the low N availability explain the dominance of small plankton groups?***

463 The single cell isotopic approach used here provides an estimate of the substrate specific uptake rate. If  
464 the only source of C for the pigmented cells is from C-fixation, C-fixation based division rates should  
465 reflect division rates at steady-state. For pigmented groups, C-fixation based division rates measured in  
466 our study (0.18-0.64  $\text{d}^{-1}$ ) are in line with previous measurements made in the N. Pacific using the same  
467 approach (0.32-0.50  $\text{d}^{-1}$ ) (Berthelot et al 2019). In our study, C-fixation based division rates were higher  
468 for *Synechococcus* ( $0.45 \pm 0.22 \text{ d}^{-1}$  on average) than for the two other pigmented groups ( $0.28 \pm 0.12 \text{ d}^{-1}$

469 on average) investigated. This is consistent with patterns and values reported in the review of Kirchman  
470 (2016).

471 While C-specific fixation did not appear to scale with cell size at the intra-group level, clear patterns  
472 were observed for N-specific uptake rates (Fig. 4). Such a relationship could be explained by nutrient  
473 availability. Under nutrient scarcity, small size plankton have a competitive advantage due to their high  
474 surface-area-to-volume ratios (Naselli-Flores et al. 2007). At the time of sampling, N species  
475 concentrations were low with the sum of  $\text{NO}_3^-$ ,  $\text{NH}_4^+$  and N-urea below  $<200 \text{ nmol N L}^{-1}$ . At such low  
476 N concentrations, the uptake is limited by the molecular diffusion of N compounds to their cellular  
477 membranes (Karp-Boss et al. 1996; Olofsson et al. 2019). Using a diffusion model (see details in  
478 Materials and Methods section), we calculated that cells with a diameter larger than  $5 \mu\text{m}$  could not  
479 maintain N-specific  $\text{NH}_4^+$  uptake as high as those measured here for pico-plankton. Similar thresholds  
480 were found for  $\text{NO}_3^-$  uptake ( $7 \mu\text{m}$ ) and N-urea uptake ( $12 \mu\text{m}$ ). Below these thresholds, smaller cells  
481 still profit from their high surface-area-to-volume ratio which could explain the overall inter- and/or  
482 intra-group patterns of increasing N-specific uptake with decreasing cell size up to  $\sim 1\text{-}2 \mu\text{m}$  equivalent  
483 spherical diameter (Fig. 4). Below this limit, the reduction in size for pigmented organisms is limited by  
484 non-scalable cellular components, in particular photosynthetic apparatus (Ward et al. 2017). The peak  
485 around  $1\text{-}2 \mu\text{m}$  equivalent spherical diameter in N-specific rates observed here for pigmented organisms  
486 is lower than a previous report in the Mediterranean lagune ( $2\text{-}3 \mu\text{m}$ ) (Bec et al. 2008). This is consistent  
487 with an adaptation of the present communities to extremely oligotrophic conditions where further cell  
488 size reduction to cope with nutrients scarcity is hindered by minimal maintenance of cellular basal  
489 functions. In the case of non-pigmented prokaryote, the more streamlined genome and metabolic  
490 functions of this group as compared to cyanobacteria and to a larger extent to photosynthetic pico-  
491 eukaryotes allow them a smaller cell size (Swan et al. 2013) and could explain their relatively high  
492 efficiency at using leucine available at extremely low concentrations in the ocean ( $<1 \text{ nM}$ , Zubkov et al  
493 2008). Taken together these observations largely explain the numerical dominance of pico-plankton in  
494 the oceanic regions sampled. It also implies that, to compensate for their lack of N acquisition  
495 competitiveness, larger photosynthetic plankton cells have to rely on alternative strategies such as

496 increasing their surface-area-to-volume ratios by developing complex nanostructure shapes (Mitchell et  
497 al. 2013), relying on predation (Stoecker et al. 2017) or symbioses with N<sub>2</sub> fixing organisms (Foster et  
498 al. 2011; Zehr et al. 2017).

#### 499 *The relative importance of organic and inorganic sources of C*

500 We measured some C-fixation for a subset of the cells of the non-pigmented prokaryotes group at all  
501 stations (15% on average, Fig. 2). This C-fixation by the non-pigmented prokaryotes group may stem  
502 from the transfer of <sup>13</sup>C fixed by the photosynthetic organisms during the incubation (Arandia-Gorostidi  
503 et al. 2017) or an active fixation performed by chemoautotrophs such as nitrifying bacteria (Middelburg  
504 2011). Despite conservative sorting procedures, it is also possible that pigmented organisms were  
505 missorted in the non-pigmented prokaryotes group. However, at the group scale, C-fixation by non-  
506 pigmented prokaryotes were not statistically significant and trivial in comparison to uptake by their  
507 photosynthetic counterparts, in line with the expected partitioning between pigmented and non-  
508 pigmented organisms with respect to C-fixation.

509 C-specific leucine potential uptake rates by non-pigmented prokaryotes were on average 4–10 times  
510 higher than those of pigmented groups (Fig. 2, Table S3) confirming the competitive advantage of  
511 heterotrophs in the acquisition of organic molecules such as leucine. C-specific leucine potential uptake  
512 rates in pigmented groups were low but statistically significant at the single cell level for 14-53% of the  
513 pigmented cells and at the group level at most sites (see criteria in material and methods section) (Table  
514 S3). This use of organic C might explain the survival of photosynthetic pico-eukaryotes in extended  
515 darkness such as polar winter (Deventer and Heckman 1996) or the maintenance of active  
516 *Prochlorococcus* populations at depth when low light levels limit photosynthetic activity (Coe et al.  
517 2016). The leucine uptake measured in pigmented groups can originate either from a direct osmotrophic  
518 uptake of leucine, or indirectly from predation on prey which would have assimilated <sup>13</sup>C-leucine during  
519 the incubation. Many studies report predation by taxa belonging to the photosynthetic pico-eukaryotes  
520 group by phagocytosis (Zubkov et al. 2008; Duhamel et al. 2019), which might explain a fraction of the  
521 leucine uptake measured here for this group. On the other hand, direct osmotrophic uptake of dissolved



522 organic compounds by pigmented eukaryotes is common and could also explain the leucine uptake  
523 observed in photosynthetic pico-eukaryotes observed in our study (Ruiz-González et al. 2012). More  
524 studies are needed to assess the relative importance of phagotrophy and osmotrophy in the mixotrophic  
525 strategies of photosynthetic pico-eukaryotes. In the cases of *Prochlorococcus* and *Synechococcus*,  
526 leucine uptake is likely through osmotrophy as direct uptake of organic molecules (e.g. glucose, amino  
527 acids) has been reported (Muñoz-Marín et al. 2020) while, to the best of our knowledge, predation has  
528 not been observed.

### 529 ***The relative importance of organic and inorganic sources of N***

530 In our study,  $\text{NH}_4^+$  and urea were the dominant sources of N at the community level (Table 1), in  
531 agreement with observations made previously in the gyre and in the Gulf Stream (Lipschultz 2001;  
532 Casey et al. 2007). This was also verified at the group level for the pigmented and non-pigmented groups  
533 (Fig. 3). The importance of  $\text{NO}_3^-$  uptake was much more reduced but contrasting patterns were observed  
534 between groups. Significant  $\text{NO}_3^-$  uptake by *Prochlorococcus* confirms previous reports (Casey et al.  
535 2007; Berube et al. 2015; Berthelot et al. 2019). However,  $\text{NO}_3^-$  only accounted for a small fraction of  
536 *Prochlorococcus* N sources ( $3.7 \pm 8.2\%$ , Table 2), in line with previous results using a similar approach  
537 in the North Pacific Gyre ( $4.5 \pm 6.5\%$ ) (Berthelot et al. 2019). In contrast,  $\text{NO}_3^-$  represented a larger  
538 fraction of N uptake for *Synechococcus* in the North Atlantic ( $11.5 \pm 12.8\%$  on average, this study) than  
539 in the North Pacific ( $2.9 \pm 2.1\%$ , Berthelot et al., 2019). This difference may be explained by the greater  
540  $\text{NO}_3^-$  concentrations in the Atlantic, since in the North Pacific Gyre, surface  $\text{NO}_3^-$  concentrations remain  
541 lower than  $10 \text{ nmol L}^{-1}$  (Karl et al. 2001). In our study regions, sampled surface waters were depleted in  
542  $\text{NO}_3^-$  but regular mixing events bring  $\text{NO}_3^-$  concentrations well above  $100 \text{ nmol L}^{-1}$  in the mixed layer,  
543 even in the GYR (Lipschultz 2001; Treibergs et al. 2014). The transiently more available  $\text{NO}_3^-$  might  
544 result in the adaptation or selection of *Synechococcus* populations that are more efficient at using  $\text{NO}_3^-$   
545 when available (Casey et al. 2007). This is further confirmed by the generally low  $\delta^{15}\text{N}$  signature of  
546 *Synechococcus* and *Prochlorococcus*, characteristic of a reliance on remineralized N compounds such  
547 as  $\text{NH}_4^+$  or N-urea (Fawcett et al. 2011). In the presence of  $\text{NO}_3^-$ , the  $\delta^{15}\text{N}$  of these groups can increase,

548 confirming the capacity of the organisms to use  $\text{NO}_3^-$  when available in the North Atlantic Gyre (Fawcett  
 549 et al. 2011; Treibergs et al. 2014).

550 Table 2. Relative importance of the different N sources investigated (average  $\pm$  standard deviation  
 551 between stations, in %) for the N acquisition budget of each group.

	Ammonium	Nitrate	N-urea	N-leucine
<b>Non-pigmented prokaryotes</b>	50.2 $\pm$ 66.2	2.1 $\pm$ 1.6	37.6 $\pm$ 28.6	10.1 $\pm$ 3.6
<i>Prochlorococcus</i>	34.3 $\pm$ 21.5	3.7 $\pm$ 8.2	61.1 $\pm$ 69.9	0.9 $\pm$ 0.4
<i>Synechococcus</i>	29.3 $\pm$ 32.4	11.5 $\pm$ 12.8	59.0 $\pm$ 54.2	0.3 $\pm$ 0.6
<b>Photosynthetic pico-eukaryotes</b>	54.7 $\pm$ 57.6	9.2 $\pm$ 10.1	35.1 $\pm$ 31.7	1.0 $\pm$ 0.6

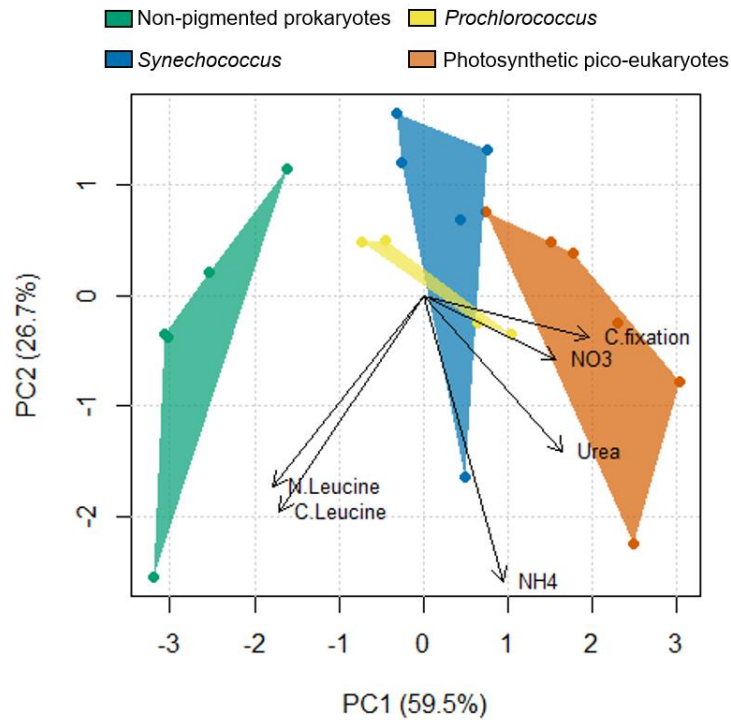
552  
 553 Pigmented organisms generally outcompeted non-pigmented prokaryotes for the acquisition of these  
 554 inorganic N species. N-specific  $\text{NH}_4^+$  and  $\text{NO}_3^-$  uptake rates by non-pigmented prokaryotes were indeed  
 555 generally lower than in pigmented groups (Fig. 3). The uptake of  $\text{NH}_4^+$  and  $\text{NO}_3^-$  by non-pigmented  
 556 prokaryotes averaged 7 $\pm$ 3% and 2 $\pm$ 2% of the community uptake, respectively. These uptake estimates  
 557 fall at the lower end of previous reported contributions ranging from 5 to 60% for  $\text{NH}_4^+$  and 4 to 80%  
 558 for  $\text{NO}_3^-$  (Kirchman et al. 1994; Fouilland et al. 2007; Trottet et al. 2011). The differences could be due  
 559 to regional variability in dissolved inorganic N concentrations, with our study sites displaying lower  
 560 concentrations than previous studies which were conducted in more N rich waters. We cannot rule out  
 561 that discrepancies also result from methodological differences, with previous studies relying mostly on  
 562 size fractionation or inhibitors. Additional single-cell experiments in N rich waters would help to unravel  
 563 changes in N-species uptake for different groups as a function of N availability.

#### 564 ***Conclusions and implications***

565 In this study, we provided a comprehensive analysis of *in situ* assimilation rates of organic and inorganic  
 566 C and N sources for different groups of the picoplankton community. A principle component analysis  
 567 shows the group specific C- and N-trophic strategies (Fig. 6). At the group level pigmented and non-  
 568 pigmented organisms were clearly partitioned, with the former clustering around C-fixation and  $\text{NO}_3^-$   
 569 and N-urea uptake, and the latter around C- and N-leucine uptake. On the other hand, the principal

570 component analysis shows that  $\text{NH}_4^+$  uptake is a poor predictor of the groups' partitions. In contrast to  
571 previous findings in the North Pacific (Berthelot et al. 2019), *Synechococcus* appeared to be the group  
572 relying the most on  $\text{NO}_3^-$ . This suggests that the same pico-plankton group might adopt different nutrient  
573 uptake strategies between oceanic regions. Intriguingly, *Prochlorococcus* and photosynthetic pico-  
574 eukaryotes showed higher C- and N-specific leucine potential uptake than *Synechococcus*. This capacity  
575 to diversify their C and N sources, either by osmotrophic uptake or by predation, may allow these  
576 microorganisms to maintain their growth under extremely severe nutrient-depleted environments  
577 (Zubkov et al. 2003). This behavior could explain the maintenance of the populations and their  
578 dominance in some of the most oligotrophic oceanic regimes (Flombaum et al. 2020).

579 Little is known on variations in nutrition acquisition strategies across environmental gradients, and in  
580 particular, across light and nutrients gradients. Taken together, our results provide a snapshot of the  
581 picoplankton strategies in the uptake of organic and inorganic sources of C and N. While we observed  
582 clear distinctions in C and N uptake strategies between pigmented and non-pigmented groups (Fig. 6),  
583 our results also highlight contrasting strategies among the pigmented groups and the importance of cell  
584 size in osmotrophic nutrient acquisition (Fig. 6). As a result of global warming, picoplankton is likely  
585 to become more important in ocean biogeochemistry as oligotrophic waters are predicted to expand due  
586 to increased water column stratification (Flombaum et al. 2020). A combination of approaches,  
587 including those presented here, will be needed to improve our understanding of the key processes (such  
588 as nutrient affinity, competition, associations, predation) determining the dynamic of plankton groups  
589 and to predict their fate in the context of a changing ocean.



590

591 *Figure 6. Principal Component Analysis of the C- and N-specific uptake rates highlighting the*  
 592 *differences in C and N strategies of the different groups investigated (data were normalized and*  
 593 *centered). Each point represents a group at a given sampling station.*

594 **Acknowledgements**

595 We would like to thank the crew of the *R/V Atlantic Explorer* for their help during the cruise. We also  
 596 thank Smail Mostefaoui for his assistance with the nanoSIMS analyses at the French National Ion  
 597 MicroProbe Facility hosted by the Muséum National d'Histoire Naturelle (Paris). N. C. and H. B. were  
 598 supported by the "Laboratoire d'Excellence" LabexMER (ANR-10-LABX-19) and co-funded by a grant  
 599 from the French government under the program "Investissements d'Avenir". SD was funded by the  
 600 National Science Foundation (OCE-1434916 and OCE-1458070).

601 **References**

- 602 Arandia-Gorostidi, N., P. K. Weber, L. Alonso-Sáez, X. A. G. Morán, and X. Mayali. 2017. Elevated  
603 temperature increases carbon and nitrogen fluxes between phytoplankton and heterotrophic  
604 bacteria through physical attachment. *ISME J.* **11**: 641–650. doi:10.1038/ismej.2016.156
- 605 Azam, F. 1998. Microbial Control of Oceanic Carbon Flux: The Plot Thickens. *Science* (80-. ). **280**:  
606 694–696. doi:10.1126/science.280.5364.694
- 607 Baer, S. E., M. W. Lomas, K. X. Terpis, C. Mouginot, and A. C. Martiny. 2017. Stoichiometry of  
608 *Prochlorococcus*, *Synechococcus*, and small eukaryotic populations in the western North Atlantic  
609 Ocean. *Environ. Microbiol.* **19**: 1568–1583. doi:10.1111/1462-2920.13672
- 610 Bec, B., Y. Collos, A. Vaquer, D. Mouillot, and P. Souchu. 2008. Growth rate peaks at intermediate  
611 cell size in marine photosynthetic picoeukaryotes. *Limnol. Oceanogr.* **53**: 863–867.  
612 doi:10.4319/lo.2008.53.2.0863
- 613 Berg, G. M., P. M. Glibert, M. W. Lomas, and M. A. Burford. 1997. Organic nitrogen uptake and  
614 growth by the chrysophyte *Aureococcus anophagefferens* during a brown tide event. *Mar. Biol.*  
615 **129**: 377–387. doi:10.1007/s002270050178
- 616 Berthelot, H., S. Duhamel, S. L’Helguen, J.-F. Maguer, S. Wang, I. Cetinić, and N. Cassar. 2019.  
617 NanoSIMS single cell analyses reveal the contrasting nitrogen sources for small phytoplankton.  
618 *ISME J.* **13**: 651–662. doi:10.1038/s41396-018-0285-8
- 619 Berube, P. M., S. J. Biller, A. G. Kent, and others. 2015. Physiology and evolution of nitrate  
620 acquisition in *Prochlorococcus*. *ISME J.* **9**: 1195–1207. doi:10.1038/ismej.2014.211
- 621 Bombar, D., R. W. Paerl, R. Anderson, and L. Riemann. 2018. Filtration via Conventional Glass Fiber  
622 Filters in <sup>15</sup>N<sub>2</sub> Tracer Assays Fails to Capture All Nitrogen-Fixing Prokaryotes. *Front. Mar. Sci.*  
623 **5**. doi:10.3389/fmars.2018.00006
- 624 Bradley, P. B., M. W. Lomas, and D. A. Bronk. 2010. Inorganic and Organic Nitrogen Use by

625 Phytoplankton Along Chesapeake Bay, Measured Using a Flow Cytometric Sorting Approach.  
626 Estuaries and Coasts **33**: 971–984. doi:10.1007/s12237-009-9252-y

627 Bronk, D. A., J. H. See, P. Bradley, and L. Killberg. 2007. DON as a source of bioavailable nitrogen  
628 for phytoplankton. Biogeosciences **4**: 283–296. doi:10.5194/bg-4-283-2007

629 Casey, J. R., K. M. Björkman, S. Ferrón, and D. M. Karl. 2019. Size dependence of metabolism within  
630 marine picoplankton populations. Limnol. Oceanogr. **64**: 1819–1827. doi:10.1002/lno.11153

631 Casey, J. R., M. W. Lomas, J. Mandecki, and D. E. Walker. 2007. *Prochlorococcus* contributes to new  
632 production in the Sargasso Sea deep chlorophyll maximum. Geophys. Res. Lett. **34**: L10604.  
633 doi:10.1029/2006GL028725

634 Coe, A., J. Ghizzoni, K. LeGault, S. Biller, S. E. Roggensack, and S. W. Chisholm. 2016. Survival of  
635 *Prochlorococcus* in extended darkness. Limnol. Oceanogr. **61**: 1375–1388.  
636 doi:10.1002/lno.10302

637 Deventer, B., and C. W. Heckman. 1996. Effects of prolonged darkness on the relative pigment  
638 content of cultured diatoms and green algae. Aquat. Sci. **58**: 241–252. doi:10.1007/BF00877511

639 Du, H., N. Jiao, Y. Hu, and Y. Zeng. 2006. Diversity and distribution of pigmented heterotrophic  
640 bacteria in marine environments. FEMS Microbiol. Ecol. **57**: 92–105. doi:10.1111/j.1574-  
641 6941.2006.00090.x

642 Duhamel, S., E. Kim, B. Sprung, and O. R. Anderson. 2019. Small pigmented eukaryotes play a major  
643 role in carbon cycling in the P-depleted western subtropical North Atlantic, which may be  
644 supported by mixotrophy. Limnol. Oceanogr. **64**: 2424–2440. doi:10.1002/lno.11193

645 Fawcett, S. E., M. W. Lomas, J. R. Casey, B. B. Ward, and D. M. Sigman. 2011. Assimilation of  
646 upwelled nitrate by small eukaryotes in the Sargasso Sea. Nat. Geosci. **4**: 717–722.  
647 doi:10.1038/ngeo1265

648 Flombaum, P., W.-L. Wang, F. W. Primeau, and A. C. Martiny. 2020. Global picophytoplankton niche

649 partitioning predicts overall positive response to ocean warming. *Nat. Geosci.* **13**: 116–120.  
650 doi:10.1038/s41561-019-0524-2

651 Foster, R. A., M. M. M. Kuypers, T. Vagner, R. W. Paerl, N. Musat, and J. P. Zehr. 2011. Nitrogen  
652 fixation and transfer in open ocean diatom-cyanobacterial symbioses. *ISME J.* **5**: 1484–93.  
653 doi:10.1038/ismej.2011.26

654 Fouilland, E., M. Gosselin, R. B. Rivkin, C. Vasseur, and B. Mostajir. 2007. Nitrogen uptake by  
655 heterotrophic bacteria and phytoplankton in Arctic surface waters. *J. Plankton Res.* **29**: 369–376.  
656 doi:10.1093/plankt/fbm022

657 Fukuda, R., H. Ogawa, T. Nagata, and I. Koike. 1998. Direct Determination of Carbon and Nitrogen  
658 Contents of Natural Bacterial Assemblages in Marine Environments. *Appl. Environ. Microbiol.*  
659 **64**: 3352–3358. doi:10.1128/AEM.64.9.3352-3358.1998

660 Gradoville, M. R., D. Bombar, B. C. Crump, R. M. Letelier, J. P. Zehr, and A. E. White. 2017.  
661 Diversity and activity of nitrogen-fixing communities across ocean basins. *Limnol. Oceanogr.*  
662 **62**: 1895–1909. doi:10.1002/lno.10542

663 Harrison, W. G., L. R. Harris, and B. D. Irwin. 1996. The kinetics of nitrogen utilization in the oceanic  
664 mixed layer: Nitrate and ammonium interactions at nanomolar concentrations. *Limnol.*  
665 *Oceanogr.* **41**: 16–32. doi:10.4319/lo.1996.41.1.0016

666 Hartmann, M., C. Grob, G. A. Tarran, A. P. Martin, P. H. Burkill, D. J. Scanlan, and M. V. Zubkov.  
667 2012. Mixotrophic basis of Atlantic oligotrophic ecosystems. *Proc. Natl. Acad. Sci.* **109**: 5756–  
668 5760. doi:10.1073/pnas.1118179109

669 Hernández-Ruiz, M., E. Barber-Lluch, A. Prieto, X. A. Álvarez-Salgado, R. Logares, and E. Teira.  
670 2018. Seasonal succession of small planktonic eukaryotes inhabiting surface waters of a coastal  
671 upwelling system. *Environ. Microbiol.* **20**: 2955–2973. doi:10.1111/1462-2920.14313

672 Hill, P. G., P. E. Warwick, and M. V. Zubkov. 2013. Low microbial respiration of leucine at ambient  
673 oceanic concentration in the mixed layer of the central Atlantic Ocean. *Limnol. Oceanogr.* **58**:

674 1597–1604. doi:10.4319/lo.2013.58.5.1597

675 Holmes, R. M., A. Aminot, R. K erouel, B. a Hooker, and B. J. Peterson. 1999. A simple and precise  
676 method for measuring ammonium in marine and freshwater ecosystems. *Can. J. Fish. Aquat. Sci.*  
677 **56**: 1801–1808. doi:10.1139/f99-128

678 Ibarbalz, F. M., N. Henry, M. C. Brand o, and others. 2019. Global Trends in Marine Plankton  
679 Diversity across Kingdoms of Life. *Cell* **179**: 1084-1097.e21. doi:10.1016/j.cell.2019.10.008

680 Jardillier, L., M. V Zubkov, J. Pearman, and D. J. Scanlan. 2010. Significant CO<sub>2</sub> fixation by small  
681 prymnesiophytes in the subtropical and tropical northeast Atlantic Ocean. *ISME J.* **4**: 1180–1192.  
682 doi:10.1038/ismej.2010.36

683 Kamjunke, N., B. K ohler, N. Wannicke, and J. Tittel. 2008. Algae as competitors for glucose with  
684 heterotrophic bacteria. *J. Phycol.* **44**: 616–623. doi:10.1111/j.1529-8817.2008.00520.x

685 Karl, D. M., K. M. Bj orkman, J. E. Dore, L. Fujieki, D. V Hebel, T. Houlihan, R. M. Letelier, and L.  
686 M. Tupas. 2001. Ecological nitrogen-to-phosphorus stoichiometry at station ALOHA. *Deep. Res.*  
687 *Part II Top. Stud. Oceanogr.* **48**: 1529–1566. doi:10.1016/S0967-0645(00)00152-1

688 Karp-Boss, L., E. Boss, and P. A. Jumars. 1996. Nutrient fluxes to planktonic osmotrophs in the  
689 presence of fluid motion. *Oceanogr. Mar. Biol. an Annu. Rev.* **34**: 71–101.

690 Kellogg, C. T. E., and J. W. Deming. 2009. Comparison of free-living, suspended particle, and  
691 aggregate-associated bacterial and archaeal communities in the Laptev Sea. *Aquat. Microb. Ecol.*  
692 doi:10.3354/ame01317

693 Kirchman, D. L., H. W. Ducklow, J. J. McCarthy, and C. Garside. 1994. Biomass and nitrogen uptake  
694 by heterotrophic bacteria during the spring phytoplankton bloom in the North Atlantic Ocean.  
695 *Deep. Res. Part I* **41**: 879–895. doi:10.1016/0967-0637(94)90081-7

696 Kirchman, D. L., and P. A. Wheeler. 1998. Uptake of ammonium and nitrate by heterotrophic bacteria  
697 and phytoplankton in the sub-Arctic Pacific. *Deep. Res. Part I Oceanogr. Res. Pap.* **45**: 347–365.



698 doi:10.1016/S0967-0637(97)00075-7

699 Klawonn, I., N. Nahar, J. Walve, and others. 2016. Cell-specific nitrogen- and carbon-fixation of  
700 cyanobacteria in a temperate marine system (Baltic Sea). *Environ. Microbiol.* **18**: 4596–4609.  
701 doi:10.1111/1462-2920.13557

702 Lee, S., Y. C. Kang, and J. A. Fuhrman. 1995. Imperfect retention of natural bacterioplankton cells by  
703 glass fiber filters. *Mar. Ecol. Prog. Ser.* doi:10.3354/meps119285

704 Li, Y. H., and S. Gregory. 1974. Diffusion of ions in sea water and in deep-sea sediments. *Geochim.*  
705 *Cosmochim. Acta* **38**: 703–714. doi:10.1016/0016-7037(74)90145-8

706 Lipschultz, F. 2001. A time-series assessment of the nitrogen cycle at BATS. *Deep. Res. Part II Top.*  
707 *Stud. Oceanogr.* **48**: 1897–1924. doi:10.1016/S0967-0645(00)00168-5

708 Longworth, L. G. 1963. Diffusion in the water-methanol system and the Walden product. *J. Phys.*  
709 *Chem.* doi:10.1021/j100797a036

710 Marañón, E. 2015. Cell Size as a Key Determinant of Phytoplankton Metabolism and Community  
711 Structure. *Ann. Rev. Mar. Sci.* **7**: 241–264. doi:10.1146/annurev-marine-010814-015955

712 Martiny, A. C., C. T. A. Pham, F. W. Primeau, J. A. Vrugt, J. K. Moore, S. A. Levin, and M. W.  
713 Lomas. 2013. Strong latitudinal patterns in the elemental ratios of marine plankton and organic  
714 matter. *Nat. Geosci.* **6**: 279–283. doi:10.1038/ngeo1757

715 Mary, I., G. A. Tarran, P. E. Warwick, M. J. Terry, D. J. Scanlan, P. H. Burkill, and M. V. Zubkov.  
716 2008. Light enhanced amino acid uptake by dominant bacterioplankton groups in surface waters  
717 of the Atlantic Ocean. *FEMS Microbiol. Ecol.* doi:10.1111/j.1574-6941.2007.00414.x

718 Massana, R. 2011. Eukaryotic Picoplankton in Surface Oceans. *Annu. Rev. Microbiol.* **65**: 91–110.  
719 doi:10.1146/annurev-micro-090110-102903

720 Middelburg, J. J. 2011. Chemoautotrophy in the ocean. *Geophys. Res. Lett.* **38**.  
721 doi:10.1029/2011GL049725

722 Mitchell, J. G., L. Seuront, M. J. Doubell, D. Losic, N. H. Voelcker, J. Seymour, and R. Lal. 2013.  
723 The Role of Diatom Nanostructures in Biasing Diffusion to Improve Uptake in a Patchy Nutrient  
724 Environment. *PLoS One*. doi:10.1371/journal.pone.0059548

725 Moore, C. M., M. M. Mills, R. Langlois, A. Milne, E. P. Achterberg, J. La Roche, and R. J. Geider.  
726 2008. Relative influence of nitrogen and phosphorus availability on phytoplankton physiology  
727 and productivity in the oligotrophic sub-tropical North Atlantic Ocean. *Limnol. Oceanogr.*  
728 doi:10.4319/lo.2008.53.1.0291

729 Moore, J. K., R. J. Geider, C. Guieu, and others. 2013. Processes and patterns of nutrient limitation.  
730 *Nat. Geosci.* **6**: 1–10. doi:10.1038/NGEO1765

731 Morán, X. A. G., J. M. Gasol, L. Arin, and M. Estrada. 1999. A comparison between glass fiber and  
732 membrane filters for the estimation of phytoplankton POC and DOC production. *Mar. Ecol.*  
733 *Prog. Ser.* doi:10.3354/meps187031

734 Moutin, T., P. Raimbault, and J.-C. Poggiale. 1999. Primary production in surface waters of the  
735 western Mediterranean sea. Calculation of daily production. *Comptes Rendus l'Académie des*  
736 *Sci. - Ser. III - Sci. la Vie* **322**: 651–659.

737 Mucko, M., S. Bosak, R. Casotti, C. Balestra, and Z. Ljubešić. 2018. Winter picoplankton diversity in  
738 an oligotrophic marginal sea. *Mar. Genomics* **42**: 14–24. doi:10.1016/j.margen.2018.09.002

739 Mulvenna, P. F., and G. Savidge. 1992. A modified manual method for the determination of urea in  
740 seawater using diacetylmonoxime reagent. *Estuar. Coast. Shelf Sci.* **34**: 429–438.  
741 doi:10.1016/S0272-7714(05)80115-5

742 Muñoz-Marín, M. C., G. Gómez-Baena, A. López-Lozano, J. A. Moreno-Cabezuelo, J. Díez, and J.  
743 M. García-Fernández. 2020. Mixotrophy in marine picocyanobacteria: use of organic compounds  
744 by *Prochlorococcus* and *Synechococcus*. *ISME J.* **14**: 1065–1073. doi:10.1038/s41396-020-0603-  
745 9

746 Naselli-Flores, L., J. Padisák, and M. Albay. 2007. Shape and size in phytoplankton ecology: do they

747 matter? *Hydrobiologia* **578**: 157–161. doi:10.1007/s10750-006-2815-z

748 Nayar, S., and L. M. Chou. 2003. Relative efficiencies of different filters in retaining phytoplankton  
749 for pigment and productivity studies. *Estuar. Coast. Shelf Sci.* doi:10.1016/S0272-  
750 7714(03)00075-1

751 Olofsson, M., E. K. Robertson, L. Edler, L. Arneborg, M. J. Whitehouse, and H. Ploug. 2019. Nitrate  
752 and ammonium fluxes to diatoms and dinoflagellates at a single cell level in mixed field  
753 communities in the sea. *Sci. Rep.* doi:10.1038/s41598-018-38059-4

754 Oremland, R. S., and D. G. Capone. 1988. Use of “Specific” Inhibitors in Biogeochemistry and  
755 Microbial Ecology, p. 285–383. *In Advances in Microbial Ecology.*

756 Otero-Ferrer, J., P. Cermeño, A. Bode, and others. 2018. Factors controlling the community structure  
757 of picoplankton in contrasting marine environments. *Biogeosciences* **15**: 6199–6220.  
758 doi:10.5194/bg-15-6199-2018

759 Raimbault, P., G. Slawyk, B. Coste, and J. Fry. 1990. Feasibility of using an automated colorimetric  
760 procedure for the determination of seawater nitrate in the 0 to 100 n M range: Examples from  
761 field and culture. *Mar. Biol.* **104**: 347–351. doi:10.1007/BF01313277

762 Ruiz-González, C., M. Galí, E. Sintes, G. J. Herndl, J. M. Gasol, and R. Simó. 2012. Sunlight Effects  
763 on the Osmotrophic Uptake of DMSP-Sulfur and Leucine by Polar Phytoplankton. *PLoS One.*  
764 doi:10.1371/journal.pone.0045545

765 Sanders, R. W., and R. J. Gast. 2012. Bacterivory by phototrophic picoplankton and nanoplankton in  
766 Arctic waters. *FEMS Microbiol. Ecol.* doi:10.1111/j.1574-6941.2011.01253.x

767 Schapira, M., C. D. McQuaid, and P. W. Froneman. 2012. Metabolism of free-living and particle-  
768 associated prokaryotes: Consequences for carbon flux around a Southern Ocean archipelago. *J.*  
769 *Mar. Syst.* doi:10.1016/j.jmarsys.2011.08.009

770 Sedwick, P. N., P. W. Bernhardt, M. R. Mulholland, R. G. Najjar, L. M. Blumen, B. M. Sohst, C.

771 Sookhdeo, and B. Widner. 2018. Assessing Phytoplankton Nutritional Status and Potential  
772 Impact of Wet Deposition in Seasonally Oligotrophic Waters of the Mid-Atlantic Bight.  
773 *Geophys. Res. Lett.* **45**: 3203–3211. doi:10.1002/2017GL075361

774 Seymour, J. R., S. A. Amin, J. B. Raina, and R. Stocker. 2017. Zooming in on the phycosphere: The  
775 ecological interface for phytoplankton-bacteria relationships. *Nat. Microbiol.*  
776 doi:10.1038/nmicrobiol.2017.65

777 Stoecker, D. K., P. J. Hansen, D. A. Caron, and A. Mitra. 2017. Mixotrophy in the Marine Plankton.  
778 *Ann. Rev. Mar. Sci.* doi:10.1146/annurev-marine-010816-060617

779 Strickland, J. D. H., and T. R. Parson. 1972. *A Practical Handbook of Seawater Analysis*, Fisheries  
780 Research Board of Canada.

781 Swan, B. K., B. Tupper, A. Sczyrba, and others. 2013. Prevalent genome streamlining and latitudinal  
782 divergence of planktonic bacteria in the surface ocean. *Proc. Natl. Acad. Sci. U. S. A.*  
783 doi:10.1073/pnas.1304246110

784 Treibergs, L. a., S. E. Fawcett, M. W. Lomas, and D. M. Sigman. 2014. Nitrogen isotopic response of  
785 prokaryotic and eukaryotic phytoplankton to nitrate availability in Sargasso Sea surface waters.  
786 *Limnol. Oceanogr.* **59**: 972–985. doi:10.4319/lo.2014.59.3.0972

787 Trottet, A., E. Fouilland, C. Leboulanger, E. Lanouguère, and M. Bouvy. 2011. Use of inhibitors for  
788 coastal bacteria and phytoplankton: Application to nitrogen uptake measurement. *Estuar. Coast.  
789 Shelf Sci.* **93**: 151–159. doi:10.1016/j.ecss.2011.04.007

790 Ward, B. A., E. Marañón, B. Sauterey, J. Rault, and D. Claessen. 2017. The size dependence of  
791 phytoplankton growth rates: A trade-off between nutrient uptake and metabolism. *Am. Nat.*  
792 doi:10.1086/689992

793 Wu, J., W. Sunda, E. A. Boyle, and D. M. Karl. 2000. Phosphate depletion in the Western North  
794 Atlantic Ocean. *Science (80-. )*. doi:10.1126/science.289.5480.759

795 Zehr, J. P., I. N. Shilova, H. M. Farnelid, M. del C. Muñoz-Marín, and K. A. Turk-Kubo. 2017.  
796 Unusual marine unicellular symbiosis with the nitrogen-fixing cyanobacterium UCYN-A. *Nat.*  
797 *Microbiol.* **2**: 16214. doi:10.1038/nmicrobiol.2016.214

798 Zubkov, M. V. 2014. Faster growth of the major prokaryotic versus eukaryotic CO<sub>2</sub> fixers in the  
799 oligotrophic ocean. *Nat. Commun.* **5**. doi:10.1038/ncomms4776

800 Zubkov, M. V., B. M. Fuchs, G. A. Tarran, P. H. Burkill, and R. Amann. 2003. High rate of uptake of  
801 organic nitrogen compounds by *Prochlorococcus* cyanobacteria as a key to their dominance in  
802 oligotrophic oceanic waters. *Appl. Environ. Microbiol.* **69**: 1299–1304.  
803 doi:10.1128/AEM.69.2.1299-1304.2003

804 Zubkov, M. V., G. A. Tarran, I. Mary, and B. M. Fuchs. 2008. Differential microbial uptake of  
805 dissolved amino acids and amino sugars in surface waters of the Atlantic Ocean. *J. Plankton Res.*  
806 **30**: 211–220. doi:10.1093/plankt/fbm091

807

808 **Supplementary Information**

809 Table S1: Minimum quantifiable rates (MQR) (as defined by Gradoville et al. 2017) of C and N  
 810 community uptake (in nmol C L<sup>-1</sup> h<sup>-1</sup> or nmol N L<sup>-1</sup> h<sup>-1</sup>) were calculated for each tracer and each  
 811 station from the propagation of errors of each parameter involved in the uptake rate calculation. For  
 812 the parameters measured in triplicate, the errors were the standard deviation. For the incubation time,  
 813 the error was estimated to be ±10 minutes (representing the typical filtration duration). For the isotopic  
 814 percent abundance of source pool during dissolved inorganic <sup>13</sup>C incubations, the error was estimated  
 815 to be ±0.5 atom%.

Station	C-fixation		Nitrate		Ammonium		Urea		C-leucine		N-leucine	
	Fixation rate	MQR	Uptake rate	MQR	Uptake rate	MQR	Uptake rate	MQR	Uptake rate	MQR	Uptake rate	MQR
A	18.7	7.2	0.4	0.3	1.0	0.5	1.0	0.6	0.2	<0.1	0.1	<0.1
B	20.2	2.4	0.4	0.1	1.7	0.3	1.8	0.4	0.2	<0.1	0.1	<0.1
C	66.7	7.5	0.9	0.1	3.0	0.6	6.3	1.0	0.4	0.1	0.1	<0.1
D	64.6	17.5	1.4	1.0	4.8	0.6	7.0	2.3	0.5	<0.1	0.2	<0.1
E	162.0	16.5	3.8	0.6	6.1	1.3	9.8	0.8	0.8	0.1	0.3	0.1
F	121.6	29.6	3.7	0.7	23.6	6.4	11.0	2.8	0.7	0.2	0.3	0.2

816

817

818

819 Table S2: Abundances of low nucleic acid content and high nucleic acid content sub-groups in the  
 820 non-pigmented prokaryote groups at each station sampled.

<b>Station</b>	<b>High nucleic acid content sub-group (10<sup>3</sup> cells ml<sup>-1</sup>)</b>	<b>Low nucleic acid content sub-group(10<sup>3</sup> cells ml<sup>-1</sup>)</b>
<b>North Atlantic Gyre</b>		
<b>A</b>	100±10	143±3
<b>B</b>	95±13	158±7
<b>Gulf Stream</b>		
<b>C</b>	404±58	181±29
<b>D</b>	214±9	167±8
<b>Continental Shelf</b>		
<b>E</b>	425±17	185±5
<b>F</b>	230±6	68±18

821

822 Table S3. C-fixation division growth rate (d<sup>-1</sup>) and C- and N-specific C-fixation, ammonium (NH<sub>4</sub><sup>+</sup>), nitrate (NO<sub>3</sub><sup>-</sup>), urea and leucine uptake rates (h<sup>-1</sup>) measured for each group  
 823 and at each station. Mean and standard deviation are in bold font. Median are in regular font and the number of cells analyzed are in italics. ND: not detected. NA: not  
 824 analyzed.

Station	Group	C-fixation based division rate (d <sup>-1</sup> )	C-specific C-fixation rates (h <sup>-1</sup> )	N-specific NH <sub>4</sub> <sup>+</sup> uptake (h <sup>-1</sup> )	N-specific NO <sub>3</sub> <sup>-</sup> uptake (h <sup>-1</sup> )	N-specific urea uptake (h <sup>-1</sup> )	C-specific leucine potential uptake (h <sup>-1</sup> )	N-specific leucine potential uptake (h <sup>-1</sup> )
A	Non-pigmented prokaryotes	ND	ND	NA	NA	<b>0.003±0.001</b> 0.003 <i>80</i>	<b>&lt;0.001±&lt;0.001</b> 0.001 <i>54</i>	<b>0.001±&lt;0.001</b> 0.001 <i>54</i>
A	<i>Prochlorococcus</i>	<b>0.25±0.26</b> 0.16 <i>171</i>	<b>0.014±0.015</b> 0.009 <i>171</i>	<b>0.012±0.004</b> 0.011 <i>47</i>	<b>&lt;0.001±&lt;0.001</b> <0.001 <i>61</i>	<b>0.004±0.005</b> 0.002 <i>63</i>	<b>&lt;0.001±&lt;0.001</b> <0.001 <i>161</i>	<b>&lt;0.001±&lt;0.001</b> <0.001 <i>161</i>
A	<i>Synechococcus</i>	<b>0.32±0.22</b> 0.25 <i>241</i>	<b>0.018±0.012</b> 0.015 <i>241</i>	<b>0.014±0.005</b> 0.013 <i>84</i>	<b>0.001±0.001</b> 0.001 <i>83</i>	<b>0.019±0.005</b> 0.019 <i>74</i>	ND	ND
A	Photosynthetic pico-eukaryotes	<b>0.20±0.19</b> 0.14 <i>149</i>	<b>0.011±0.011</b> 0.008 <i>149</i>	NA	<b>&lt;0.001±&lt;0.001</b> <0.001 <i>77</i>	<b>0.002±0.002</b> 0.002 <i>72</i>	<b>&lt;0.001±&lt;0.001</b> <0.001 <i>63</i>	<b>&lt;0.001±&lt;0.001</b> <0.001 <i>63</i>
B	Non-pigmented prokaryotes	ND	ND	<b>0.003±0.001</b> 0.003 <i>42</i>	<b>0.001±&lt;0.001</b> <0.001 <i>75</i>	<b>0.004±0.001</b> 0.004 <i>67</i>	<b>&lt;0.001±&lt;0.001</b> <0.001 <i>131</i>	<b>0.001±&lt;0.001</b> 0.002 <i>131</i>
B	<i>Prochlorococcus</i>	<b>0.18±0.09</b> 0.17 <i>335</i>	<b>0.010±0.005</b> 0.10 <i>335</i>	<b>0.010±0.003</b> 0.009 <i>111</i>	<b>&lt;0.001±&lt;0.001</b> <0.001 <i>92</i>	<b>0.019±0.011</b> 0.019 <i>132</i>	<b>&lt;0.001±&lt;0.001</b> <0.001 <i>77</i>	<b>&lt;0.001±0.001</b> <0.001 <i>77</i>
B	<i>Synechococcus</i>	<b>0.25±0.15</b> 0.20 <i>226</i>	<b>0.014±0.009</b> 0.012 <i>226</i>	<b>0.010±0.004</b> 0.009 <i>96</i>	<b>0.009±0.003</b> 0.009 <i>40</i>	<b>0.031±0.011</b> 0.030 <i>90</i>	ND	ND
B	Photosynthetic pico-eukaryotes	<b>0.34±0.23</b> 0.28 <i>254</i>	<b>0.019±0.012</b> 0.016 <i>254</i>	<b>0.006±0.003</b> 0.006 <i>126</i>	<b>0.001±0.002</b> <0.001 <i>80</i>	<b>0.002±0.002</b> 0.002 <i>48</i>	<b>&lt;0.001±&lt;0.001</b> <0.001 <i>72</i>	<b>&lt;0.001±0.001</b> <0.001 <i>72</i>
C	Non-pigmented prokaryotes	ND	ND	<b>0.003±0.002</b> 0.002 <i>102</i>	<b>&lt;0.001±&lt;0.001</b> <0.001 <i>98</i>	<b>0.005±0.005</b> 0.004 <i>44</i>	<b>&lt;0.001±&lt;0.001</b> <0.001 <i>74</i>	<b>0.001±&lt;0.001</b> 0.002 <i>74</i>
C	<i>Prochlorococcus</i>	<b>0.39±0.16</b> 0.38 <i>192</i>	<b>0.021±0.008</b> 0.021 <i>192</i>	<b>0.010±0.002</b> 0.011 <i>59</i>	<b>0.004±0.005</b> 0.001 <i>61</i>	<b>0.042±0.011</b> 0.044 <i>72</i>	<b>&lt;0.001±&lt;0.001</b> <0.001 <i>93</i>	<b>&lt;0.001±&lt;0.001</b> <0.001 <i>93</i>
C	<i>Synechococcus</i>	<b>0.45±0.22</b> 0.52 <i>219</i>	<b>0.023±0.011</b> 0.027 <i>219</i>	<b>0.018±0.003</b> 0.018 <i>56</i>	<b>0.012±0.004</b> 0.013 <i>69</i>	<b>0.024±0.016</b> 0.026 <i>94</i>	<b>&lt;0.001±&lt;0.001</b> <0.001 <i>13</i>	<b>&lt;0.001±&lt;0.001</b> <0.001 <i>13</i>
C	Photosynthetic pico-eukaryotes	<b>0.22±0.18</b> 0.18 <i>219</i>	<b>0.012±0.009</b> 0.010 <i>219</i>	<b>0.002±0.002</b> 0.002 <i>64</i>	<b>0.002±0.003</b> <0.001 <i>103</i>	<b>0.005±0.005</b> 0.004 <i>52</i>	<b>&lt;0.001±&lt;0.001</b> <0.001 <i>118</i>	<b>&lt;0.001±&lt;0.001</b> <0.001 <i>118</i>



<b>D</b>	<b>Non-pigmented prokaryotes</b>	ND	ND	<b>0.004±0.002</b> 0.004 36	<b>ND</b>	<b>0.001±0.001</b> 0.001 76	<b>&lt;0.001±&lt;0.001</b> <0.001 68	<b>0.002±&lt;0.001</b> 0.001 68
<b>D</b>	<i>Prochlorococcus</i>	<b>0.35±0.16</b> 0.37 224	<b>0.020±0.009</b> 0.022 224	<b>0.020±0.007</b> 0.019 98	<b>0.001±0.001</b> <0.001 73	<b>0.027±0.013</b> 0.030 53	<b>&lt;0.001±&lt;0.001</b> <0.001 63	<b>&lt;0.001±&lt;0.001</b> <0.001 63
<b>D</b>	<i>Synechococcus</i>	<b>0.64±0.42</b> 0.66 171	<b>0.034±0.021</b> 0.037 171	<b>0.017±0.013</b> 0.015 57	<b>0.006±0.003</b> 0.006 70	<b>0.060±0.018</b> 0.065 44	<b>&lt;0.001±&lt;0.001</b> <0.001 65	<b>&lt;0.001±&lt;0.001</b> <0.001 65
<b>D</b>	<b>Photosynthetic pico-eukaryotes</b>	<b>0.34±0.23</b> 0.32 274	<b>0.019±0.011</b> 0.019 274	<b>0.019±0.012</b> 0.019 111	<b>0.001±0.001</b> <0.001 123	<b>0.003±0.004</b> 0.001 40	<b>&lt;0.001±&lt;0.001</b> <0.001 84	<b>&lt;0.001±&lt;0.001</b> <0.001 84
<b>E</b>	<b>Non-pigmented prokaryotes</b>	ND	ND	<b>0.002±0.001</b> 0.002 62	<b>&lt;0.001±&lt;0.001</b> <0.001 98	<b>0.004±0.002</b> 0.004 61	<b>&lt;0.001±&lt;0.001</b> 0.002 59	<b>0.001±&lt;0.001</b> 0.001 59
<b>E</b>	<i>Prochlorococcus</i>	ND	ND	ND	ND	ND	ND	ND
<b>E</b>	<i>Synechococcus</i>	<b>0.52±0.15</b> 0.53 318	<b>0.028±0.007</b> 0.029 318	<b>0.010±0.002</b> 0.010 137	<b>0.005±0.002</b> 0.005 124	<b>0.033±0.014</b> 0.037 57	<b>&lt;0.001±&lt;0.001</b> <0.001 48	<b>&lt;0.001±&lt;0.001</b> <0.001 48
<b>E</b>	<b>Photosynthetic pico-eukaryotes</b>	<b>0.24±0.12</b> 0.23 232	<b>0.013±0.007</b> 0.013 232	<b>0.001±0.002</b> <0.001 14	<b>0.007±0.004</b> 0.008 114	<b>0.019±0.014</b> 0.016 104	<b>&lt;0.001±&lt;0.001</b> <0.001 142	<b>&lt;0.001±&lt;0.001</b> <0.001 142
<b>F</b>	<b>Non-pigmented prokaryotes</b>	ND	ND	<b>0.021±0.006</b> 0.020 115	<b>0.001±&lt;0.001</b> 0.001 61	<b>0.012±0.006</b> 0.011 40	<b>0.001±&lt;0.001</b> 0.001 51	<b>0.002±0.001</b> 0.002 51
<b>F</b>	<i>Prochlorococcus</i>	ND	ND	ND	ND	ND	ND	ND
<b>F</b>	<i>Synechococcus</i>	<b>0.51±0.25</b> 0.57 244	<b>0.027±0.013</b> 0.031 244	<b>0.035±0.017</b> 0.036 106	<b>0.009±0.004</b> 0.009 83	<b>0.046±0.011</b> 0.049 55	<b>0.001±&lt;0.001</b> <0.001 54	<b>&lt;0.001±0.001</b> <0.001 54
<b>F</b>	<b>Photosynthetic pico-eukaryotes</b>	<b>0.28±0.18</b> 0.26 360	<b>0.016±0.010</b> 0.014 360	<b>0.038±0.019</b> 0.035 98	<b>0.003±0.003</b> 0.001 137	<b>0.020±0.012</b> 0.017 125	<b>0.001±&lt;0.001</b> <0.001 46	<b>0.001±0.001</b> <0.001 46

826 Table S4: Cell-specific C-fixation rates and ammonium (NH<sub>4</sub><sup>+</sup>), nitrate (NO<sub>3</sub><sup>-</sup>), N-urea, C-leucine, N-  
 827 leucine uptake rates (average of cells analyzed, in amol C cell<sup>-1</sup> h<sup>-1</sup> and amol N cell<sup>-1</sup> h<sup>-1</sup>) at the  
 828 sampled stations. ND: not detected. NA: not analyzed.

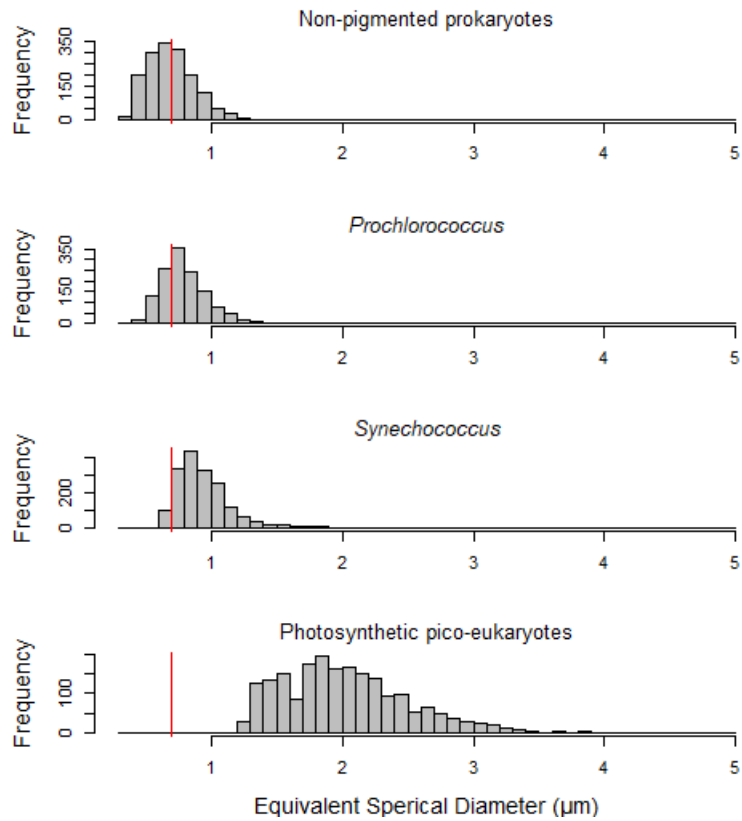
Station	Cell-specific C-fixation	Cell-specific NH <sub>4</sub> <sup>+</sup> uptake	Cell-specific NO <sub>3</sub> <sup>-</sup> uptake	Cell-specific N-Urea uptake	Cell-specific C-leucine potential uptake	Cell-specific N-leucine potential uptake
<b>Non-pigmented prokaryote</b>						
A	ND	NA	NA	0.7±0.3	0.8±0.2	0.3±0.1
B	ND	0.8±0.2	0.1±<0.1	1.1±0.2	0.7±0.3	0.4±0.1
C	ND	0.6±0.5	<0.1	1.2±1.2	0.2±0.2	0.2±0.1
D	ND	1.0±0.5	<0.1	0.4±0.3	0.7±0.2	0.4±0.1
E	ND	0.4±0.2	0.1±<0.1	1.1±0.4	0.6±0.2	0.3±0.1
F	ND	5.3±1.6	0.1±<0.1	2.9±1.4	1.1±0.4	0.5±0.1
<b><i>Prochlorococcus</i></b>						
A	69.5±73.2	7.5±2.9	0.2±0.3	2.9±3.1	0.9±1.1	0.3±0.3
B	50.6±26.9	6.2±1.7	0.3±0.3	12.3±7.1	0.6±1.3	0.3±0.4
C	101.8±38.4	7.0±1.3	2.7±3.4	27.4±7.4	1.0±0.5	0.2±0.1
D	97.9±44.0	13.1±4.3	0.4±0.8	17.7±8.4	0.5±0.5	0.2±0.2
<b><i>Synechococcus</i></b>						
A	419.1±283.7	32.9±11.2	3.4±2.9	44.2±10.8	ND	ND
B	317.3±196.6	24.1±9.7	20.2±7.1	73.9±25.4	ND	ND
C	558.4±244.8	44.1±7.0	28.4±9.2	56.1±36.3	0.6±1.8	0.3±0.4
D	806.3±476.9	41.8±31.6	13.5±6.5	143.4±43.1	0.5±1.1	0.3±0.3
E	618.4±160.1	24.5±4.3	12.0±5.0	77.5±33.6	0.5±2.2	0.2±0.3
F	645.4±292.2	83.0±40.4	20.9±9.4	109.8±25.1	3.3±8.7	1.2±1.6
<b>Photosynthetic pico-eukaryotes</b>						
A	2871.6±2846.0	NA	3.3±6.5	55.7±55.6	24.8±21.1	6.5±5.7
B	4968.5±3122.3	132.8±79.6	22.1±41.1	47.3±45.0	16.5±40.6	8.7±12.3
C	2886.8±2411.4	58.0±47.0	38.4±63.2	119.0±116.6	10.1±19.5	3.1±5.0

---

<b>D</b>	5387.9±2811.5	449.0±277.8	13.8±18.0	66.7±86.1	3.5±23.8	2.8±5.7
<b>E</b>	3056.0±1689.5	27.4±42.1	174.1±93.8	437.2±326.6	4.4±12.2	1.6±1.7
<b>F</b>	4098.8±2520.2	878.5±440.7	59.6±80.9	466.6±289.4	50.0±62.4	11.8±12.6

---

829



830

831

832

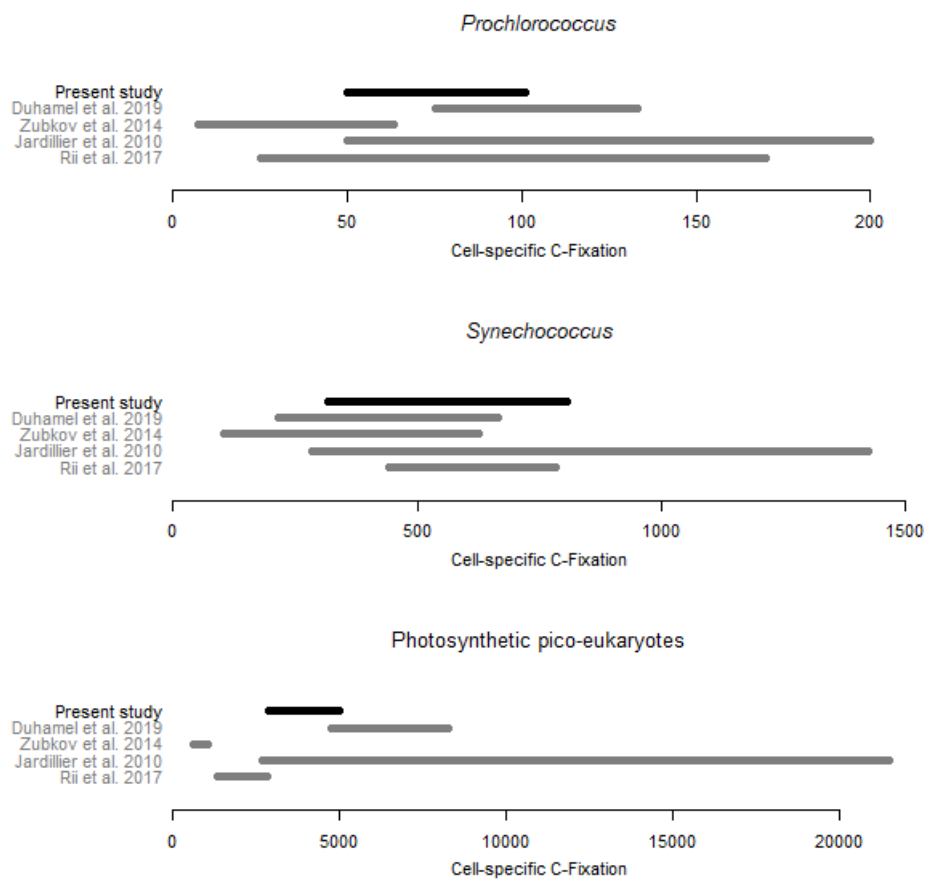
833

834

835

836

Fig S1. Frequency plot of the equivalent spherical diameter ( $\mu\text{m}$ ) of the regions of interest (cells) measured for each group. The red vertical lines depict the nominal pore size of the GF/F filters ( $0.7 \mu\text{m}$ ). 54%, 31%, 7% and 0% of the non-pigmented prokaryotes, *Prochlorococcus*, *Synechococcus* and photosynthetic pico-eukaryotes cells, respectively, were smaller than  $0.7 \mu\text{m}$ . Note that only low nucleic acid non-pigmented prokaryotes were analyzed. It is likely that the equivalent spherical diameter of the high nucleic acid non-pigmented prokaryotes was higher.



837

838 Fig S2. Compilation of the cell-specific C-fixation rates (in amol C cell<sup>-1</sup> h<sup>-1</sup>) available in the literature  
 839 for *Prochlorococcus*, *Synechococcus* and photosynthetic pico-eukaryotes.